

Recovered finite element methods on polygonal and polyhedral meshes

Zhaonan Dong*

Emmanuil H. Georgoulis[†]

Tristan Pryer[‡]

April 24, 2018

Abstract

Recovered finite element methods (R-FEM) has been recently introduced in [21] for meshes consisting of simplicial and/or box-type meshes. Here, utilising the flexibility of R-FEM framework, we extend their definition on polygonal and polyhedral meshes in two and three spatial dimensions, respectively. A key attractive feature of this framework is its ability to produce *conforming* discretizations, yet involving *only* as many degrees of freedom as discontinuous Galerkin methods over general polygonal/polyhedral meshes with potentially many faces per element. A priori error bounds are shown for general linear, possibly degenerate, second order advection-diffusion-reaction boundary value problems. A series of numerical experiments highlights the good practical performance of the proposed numerical framework.

1 Introduction

Recently, there has been a considerable interest in the construction of Galerkin-type numerical methods over meshes consisting of general polygons in two dimensions or general polyhedra in three dimensions, henceforth termed collectively as *polytopic*, as opposed to the classical Galerkin methods employing simplicial and/or box-type meshes. This interest is predominantly motivated by the potential reduction in the total numerical degrees of freedom required for the numerical solution of PDE problems. This is particularly pertinent in the context of adaptive computations for evolution PDE problems, where dynamic mesh modification is widely accepted as a promising tool for the reduction of computational complexity in both Eulerian and Lagrangian contexts. Galerkin procedures over polytopic meshes have been also proposed in the context of interface problems (porosity profiles, interfaces, etc.), as well as in the context of coarse correction computations in multilevel solvers for elliptic boundary-value problems.

Popular polytopic methods include the virtual element method [2, 10], which is itself an evolution of the so-called mimetic finite difference methods [1], polygonal finite element methods [34], composite finite element methods [23, 31] and various discontinuous Galerkin (dG) approaches, ranging from one-field interior penalty dG methods [16, 9, 7, 8], to hybridized formulations [15, 14]. DG methods are attractive as one can control the number the global numerical degrees of freedom independently of the mesh topology (i.e., the connectivity of

*Department of Mathematics, University of Leicester, University Road, Leicester LE1 7RH, UK zd14@le.ac.uk.

[†]Department of Mathematics, University of Leicester, University Road, Leicester LE1 7RH, UK and School of Applied Mathematical and Physical Sciences, National Technical University of Athens, Zografou 15780, Greece Emmanuil.Georgoulis@le.ac.uk.

[‡]Department of Mathematics and Statistics, University of Reading, Whiteknights, PO Box 220, Reading RG6 6AX, UK T.Pryer@reading.ac.uk.

the nodes/faces/elements), whereas polygonal finite elements and virtual element methods are attractive as they involve conforming approximation spaces. To construct such conforming spaces, polygonal finite element and/or virtual element methods involve basis functions which are dependent on the mesh topology: roughly speaking, even the lowest order spaces require as many basis functions as the number of mesh nodes, thereby hindering a potential substantial complexity reduction by the use of polytopic elements with “many” faces.

In this work, motivated by the recent recovered finite element framework presented in [21], we construct *conforming* methods over polytopic meshes whose set of degrees of freedom is *independent* of the number of vertices/edges/faces of each element. The proposed method depends, instead, on the choice of a sub-triangulation of the polytopic meshes. Crucially, however, the computational complexity of the method is *independent* of the cardinality of the simplices in the sub-triangulation. More specifically, the recovered finite element method (R-FEM) on polytopic meshes combines completely discontinuous local *polynomial* spaces, resulting, nonetheless, to conforming approximations.

To fix ideas, let us consider an elliptic boundary value problem with homogeneous Dirichlet boundary conditions. Let $\mathcal{E} : V_h \rightarrow \tilde{V}_h \cap H_0^1(\Omega)$ an operator mapping a *discontinuous* element-wise polynomial space V_h over a polytopic mesh onto a space of *continuous* piecewise polynomial space $\tilde{V}_h \cap H_0^1(\Omega)$ over a, generally speaking, finer simplicial mesh arising from a sub-triangulation of the polytopic mesh; such *recovery* operators \mathcal{E} can be constructed locally, e.g., by (weighted) averaging of the nodal degrees of freedom [27, 12]. We can now consider the method: find $u_h \in V_h$, such that

$$\int_{\Omega} \nabla \mathcal{E}(u_h) \cdot \nabla \mathcal{E}(v_h) dx + s(u_h, v_h) = \int_{\Omega} f \mathcal{E}(v_h) dx, \quad \text{for all } v_h \in V_h,$$

for $f \in H^{-1}(\Omega)$ and a suitable *stabilization* $s(\cdot, \cdot) : V_h \times V_h \rightarrow \mathbb{R}$, whose functionality is the treatment of the kernel $\{0 \neq v_h \in V_h : \mathcal{E}(v_h) = 0\}$ to achieve unisolvence. Crucially, despite using element-wise discontinuous polynomial trial and test space V_h , the method also produces simultaneously a conforming approximation $\mathcal{E}(u_h)$. We note that the above method yields, in general, different numerical solutions to those one would get by postprocessing standard dG approximations on polytopic meshes via the recovery operator \mathcal{E} . In the limit case of the above R-FEM posed on a simplicial mesh (rather than a general polytopic one), $\mathcal{E}(u_h)$ corresponds to the classical conforming FEM approximations for certain choices of \mathcal{E} [21]. Therefore, in this sense, R-FEM is an extension of classical finite element methods to polytopic meshes. An interesting property of the proposed method is that the user has access to the computed approximate solution at every point in the computational domain. This may be of practical interest both in the context of further post-processing and in the visualisation of the computation on standard widely available software.

The above example of an elliptic problem is intended to highlight some of the attractive features for R-FEM: a) conformity is not hard-wired in the approximation spaces and b) there is considerable flexibility in the particular choice of the recovery operator \mathcal{E} , the finite element space $\mathcal{E}(V_h)$, and the stabilisation s used. Moreover, since $\{0 \neq v_h \in V_h : \mathcal{E}(v_h) = 0\}$ is allowed to be *non-trivial* by construction, R-FEM offers significant flexibility in combining various types of numerical degrees of freedom (nodal, modal, moments, etc.) for different elements in the same mesh. This may be of interest in the treatment of interface problems.

The remainder of this work is structured as follows. In Section 2, we introduce the problem and define a set of polytopic meshes. In Section 3, we introduce the FEM spaces and the recovery operators. Section 4 presents the concepts and ideas for designing R-FEM. In Section 5, we define the R-FEM for the model problem. The a priori error analysis for R-FEM is presented in Section 6. Finally, the practical performance of the proposed R-FEM is tested

through a series of numerical examples in Section 7.

2 Model problem

Throughout this work we denote the standard Lebesgue spaces by $L^p(\omega)$, $1 \leq p \leq \infty$, $\omega \subset \mathbb{R}^d$, $d = 2, 3$, with corresponding norms $\|\cdot\|_{L^p(\omega)}$; the norm of $L^2(\omega)$ will be denoted by $\|\cdot\|_\omega$ for brevity. Let also $W^{s,p}(\omega)$ and $H^s(\omega) := W^{s,2}(\omega)$, be the Banach and Hilbertian Sobolev space of index $s \in \mathbb{R}$ of real-valued functions defined on $\omega \subset \mathbb{R}^d$, respectively, constructed via standard interpolation and/or duality procedures for $s \notin \mathbb{N}_0$. For $H^s(\omega)$, we denote the corresponding norm and seminorm by $\|\cdot\|_{s,\omega}$ and $|\cdot|_{s,\omega}$, respectively. We also denote by $H_0^1(\omega)$ the space of functions in $H^1(\omega)$ with vanishing trace on $\partial\omega$.

For Ω a bounded open polygonal domain in \mathbb{R}^d , $d \in \mathbb{N}$, with $\partial\Omega$ denoting its boundary, we consider advection-diffusion-reaction problem

$$-\nabla \cdot a \nabla u + \mathbf{b} \cdot \nabla u + cu = f \quad \text{in } \Omega, \quad (1)$$

where $f \in L^2(\Omega)$, $\mathbf{b} \in [W^{1,\infty}(\Omega)]^d$, $c \in L^\infty(\Omega)$, for some definite diffusion tensor $a \in [L^\infty(\Omega)]^{d \times d}$ satisfying

$$\zeta^T a(x) \zeta \geq 0, \quad \text{for all } \zeta \in \mathbb{R}^d, \quad (2)$$

for almost every $x \in \bar{\Omega}$. This class of problem is often termed *PDEs with non-negative characteristic form* [29] and includes elliptic, parabolic, first order hyperbolic as well as other non-standard types of PDEs, such as ultra-parabolic and various classes of linear degenerate equations. In particular, the important family of linear Kolmogorov-Fokker-Planck equations are of the form (1).

To prescribe suitable boundary conditions, we begin by splitting $\partial\Omega$ into

$$\Gamma_0 := \{x \in \partial\Omega : \mathbf{n}^T(x) a(x) \mathbf{n}(x) > 0\},$$

and

$$\Gamma_1 := \{x \in \partial\Omega : \mathbf{n}^T(x) a(x) \mathbf{n}(x) = 0\},$$

with $\mathbf{n}(x)$ denoting the unit outward normal vector to Ω at $x \in \partial\Omega$; the latter is further subdivided into inflow

$$\Gamma_- := \{x \in \Gamma_1 : \mathbf{b}(x) \cdot \mathbf{n}(x) < 0\},$$

and outflow $\Gamma_+ := \Gamma_0 \setminus \Gamma_-$ parts of the boundary. The “elliptic” part of the boundary Γ_0 , is subdivided into Γ_D and Γ_N , on which we can prescribe Dirichlet and Neumann boundary conditions, respectively. For simplicity, we assume that $|\Gamma_D| > 0$, with $|\cdot|$ denoting the Hausdorff measure with the dimension of its argument, and that $\mathbf{b}(x) \cdot \mathbf{n}(x) \geq 0$ for almost all $x \in \Gamma_N$. To complete the problem, we impose the boundary conditions:

$$\begin{aligned} u &= g_D, & \text{on } \Gamma_D \cup \Gamma_-, \\ a \nabla u \cdot \mathbf{n} &= g_N, & \text{on } \Gamma_N, \end{aligned} \quad (3)$$

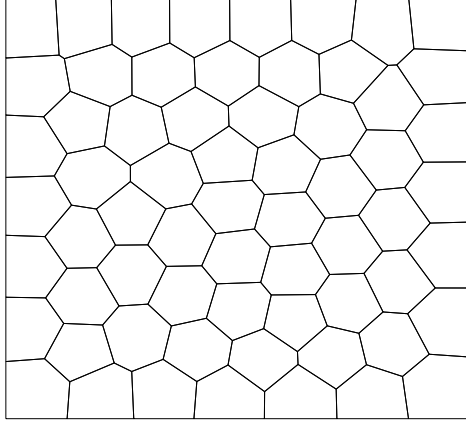
for some known $g_D \in L^2(\partial\Omega)$ and $g_N \in H^{1/2}(\partial\Omega)$. For convenience, we also define the set

$$\Gamma_D^- := \{x \in \partial\Omega : \mathbf{b}(x) \cdot \mathbf{n}(x) < 0\},$$

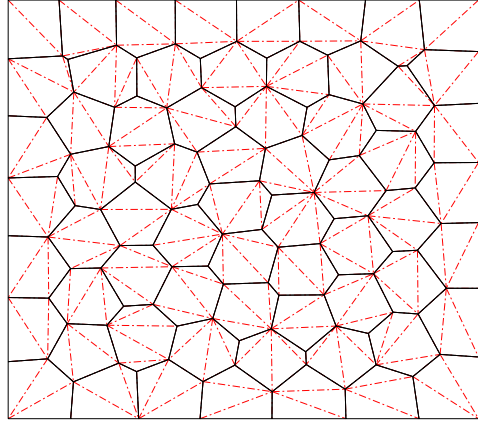
i.e., the inflow part of the boundary including also, possibly, points of Γ_D . Similarly, we define $\Gamma_N^+ = \partial\Omega \setminus \Gamma_D^-$. Additionally, we assume that the following positivity hypothesis holds: there exists a positive constant γ_0 such that

$$c_0(x) := c(x) - \frac{1}{2} \nabla \cdot \mathbf{b}(x) \geq \gamma_0 \quad \text{a.e. } x \in \Omega. \quad (4)$$

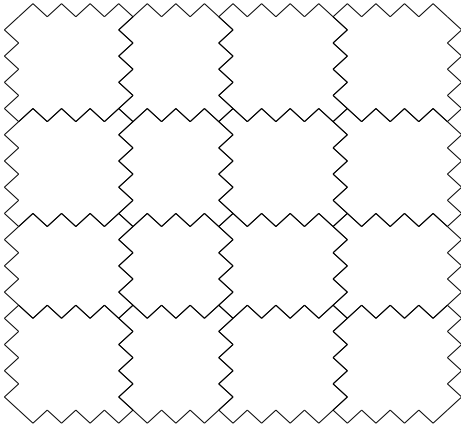
The well-posedness of the boundary value problem (1), (3) has been studied in [24].



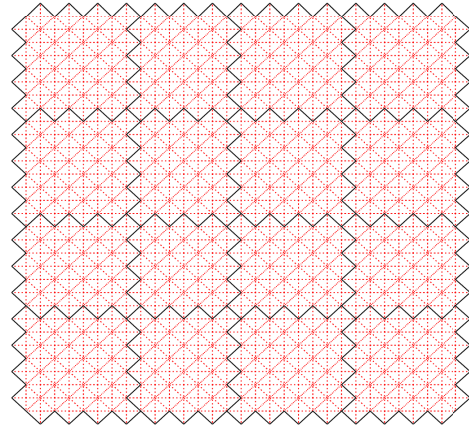
(a) A polygonal mesh \mathcal{T}_1 .



(b) A simplicial subdivision $\tilde{\mathcal{T}}_1$.



(c) An example of an agglomerated mesh with many tiny faces \mathcal{T}_2 .



(d) A simplicial background mesh $\tilde{\mathcal{T}}_2$.

Figure 1: Two examples of a polygonal meshes and respective simplicial subdivisions.

3 Finite element spaces and recovery operators

Let \mathcal{T} be a subdivision of Ω into disjoint polygonal elements for $d = 2$ or to disjoint polyhedral elements for $d = 3$; henceforth, these will be collectively referred to as *polytopic elements*. For simplicity, we assume that the subdivision \mathcal{T} can be further subdivided into a regular (i.e., no hanging nodes) and shape-regular simplicial triangulation $\tilde{\mathcal{T}}$ (see, e.g., p.124 in [11]), that $\bar{\Omega} = \cup_{T \in \mathcal{T}} \bar{T}$. Such a setting can be constructed, e.g., by agglomerating simplicial elements into polytopic ones.

By Γ we shall denote the union of all $(d-1)$ -dimensional faces associated with the subdivision \mathcal{T} including the boundary. Further, we set $\Gamma_{\text{int}} := \Gamma \setminus \partial\Omega$. Correspondingly, we define $\tilde{\Gamma}$ and $\tilde{\Gamma}_{\text{int}}$ for $\tilde{\mathcal{T}}$. Note that, by construction, $\Gamma \subset \tilde{\Gamma}$ and $\Gamma_{\text{int}} \subset \tilde{\Gamma}_{\text{int}}$.

For a nonnegative integer r , we denote the set of all polynomials of total degree at most r by $\mathcal{P}_r(T)$. For $r \geq 1$, we consider the finite element space

$$V_h^r := \{v \in L^2(\Omega) : v|_T \in \mathcal{P}_r(T), T \in \mathcal{T}\}. \quad (5)$$

We stress that V_h^r is element-wise discontinuous polynomial with respect to the *polytopic* mesh \mathcal{T} ; in this context, the dimension of V_h^r coincides with the dimension of discontinuous Galerkin finite element spaces on polytopic meshes, cf., [9, 7, 6]. In particular, the dimension of V_h^r is

not dependent on the number of vertices of the mesh \mathcal{T} . Correspondingly, we define

$$\tilde{V}_h^r := \{v \in L^2(\Omega) : v|_T \in \mathcal{P}_r(T), T \in \tilde{\mathcal{T}}\},$$

the respective discontinuous polynomial space on the sub-triangulation $\tilde{\mathcal{T}}$. Note that $V_h^r \subset \tilde{V}_h^r$.

Further, let $T^+, T^- \in \mathcal{T}$ be two (generic) elements sharing a facet $e := \partial T^+ \cap \partial T^- \subset \Gamma_{\text{int}}$ with respective outward normal unit vectors \mathbf{n}^+ and \mathbf{n}^- on e . For a function $v : \Omega \rightarrow \mathbb{R}$ that may be discontinuous across Γ_{int} , we set $v^+ := v|_{e \subset \partial T^+}$, $v^- := v|_{e \subset \partial T^-}$, and we define the jump and average by

$$[v] := v^+ \mathbf{n}^+ + v^- \mathbf{n}^- \quad \text{and} \quad \{v\} := \frac{1}{2}(v^+ + v^-);$$

if $e \in \partial T \cap \partial \Omega$, we set $[v] := v^+ \mathbf{n}$. Also, we define $h_T := \text{diam}(T)$ and we set $\mathbf{h} : \Omega \setminus \Gamma \rightarrow \mathbb{R}$, with $\mathbf{h}|_T = h_T$, $T \in \mathcal{T}$. Similarly, we set $\tilde{\mathbf{h}}$ for the meshsize function of $\tilde{\mathcal{T}}$. Throughout this work, we assume that the families of meshes considered in this work are locally quasi-uniform and that there exists constant $c_\Delta > 1$, independent of the meshsizes such that

$$c_\Delta^{-1} \mathbf{h} \leq \tilde{\mathbf{h}} \leq c_\Delta \mathbf{h},$$

uniformly as $\mathbf{h} \rightarrow 0$. Moreover, for the restriction a function v on an element $T \in \mathcal{T}$, $v|_T : T \rightarrow \mathbb{R}$, which may be discontinuous across ∂T , we shall use the notational convention that $v^+|_{\partial T}$ signifies the trace from within T while $v^-|_{\partial T}$ signifies the trace from within $\Omega \setminus T$. Using this convention we also define the *signed jump* (also known as *upwind* jump in the discontinuous Galerkin literature) on each face e by

$$[v]|_e := v^+|_e - v^-|_e;$$

note that $|[v]| = |[v]|$, i.e., the two jump notions can differ at most up to a sign on each face.

Also, we shall denote by $\partial_- T$ and by $\partial_+ T$ the *inflow* and *outflow* parts of the boundary of an element T , defined as

$$\partial_- T := \{x \in \partial T : \mathbf{b}(x) \cdot \mathbf{n}(x) < 0\} \quad \text{and} \quad \partial_+ T := \{x \in \partial T : \mathbf{b}(x) \cdot \mathbf{n}(x) > 0\},$$

respectively.

For the definition of the proposed method, we shall require a *recovery operator* of the form

$$\mathcal{E} : V_h^r \rightarrow V \cap \tilde{V}_h^r, \tag{6}$$

for some non-negative integer r , mapping element-wise discontinuous functions into functions in the solution space for the boundary value problem V , for some $r \in \mathbb{N} \cup \{0\}$. When the diffusion tensor a is strictly positive definite (i.e., when (2) holds with strict inequality) we may take $V = H^1(\Omega)$.

Recovery operators of the form (6) have appeared in various settings in the theory of finite element methods, e.g., [12, 33, 30, 27, 3, 19]. They are typically used to recover a “conforming” function from a “non-conforming” one, often under minimal regularity requirements.

A popular and very practical example for \mathcal{E} is the nodal *averaging operator* for which the following celebrated stability result was proven by Karakashian and Pascal in [27].

Lemma 3.1 *Let \mathcal{T} a polytopic mesh and $\tilde{\mathcal{T}}$ its related sub-triangulation satisfying the above assumptions. Denoting by \mathcal{N} the set of all Lagrange nodes of $\tilde{V}_h^r \cap H^1(\Omega)$, the operator $\mathcal{E}_r : V_h^r \rightarrow \tilde{V}_h^r \cap H^1(\Omega)$ is defined by:*

$$\mathcal{E}_r(v)(\nu) := \frac{1}{|\omega_\nu|} \sum_{T \in \omega_\nu} v|_T(\nu),$$

with $\omega_\nu := \bigcup_{T \in \mathcal{T}: \nu \in \bar{T}} T$, the set of elements sharing the node $\nu \in \mathcal{N}$ and $|\omega_\nu|$ their cardinality. Then, the following bound holds

$$\sum_{T \in \mathcal{T}} |v - \mathcal{E}_r(v)|_{\alpha, T}^2 \leq C_{|\alpha|} \|\mathbf{h}^{1/2-\alpha}[v]\|_{\Gamma_{\text{int}}}^2, \quad (7)$$

with $|\alpha| \in \mathbb{N} \cup \{0\}$, $C_{|\alpha|} \equiv C_{|\alpha|}(r) > 0$ a constant independent of \mathbf{h} , v and $\tilde{\mathcal{T}}$, but depending on the shape-regularity of $\tilde{\mathcal{T}}$, on c_Δ , and on the polynomial degree r .

Proof. See Karakashian and Pascal [27]. □

The bound (7) shows, in particular, that $\|\mathbf{h}^{-1/2}[v]\|_{\Gamma_{\text{int}}}^2$ is a norm on the orthogonal complement W_h^r of $\tilde{V}_h^r \cap H^1(\Omega)$ in V_h^r with respect to the standard H^1 -inner product.

Remark 3.2 *It is possible to make a number of different choices*

$$\mathcal{E} : V_h^r \rightarrow V \cap \hat{V}_h^s, \quad (8)$$

for instance, for \hat{V}_h^s say a non-conforming finite element space, e.g., Crouzeix-Raviart elements and s may be in general different to r . Indeed, various choices of \mathcal{E} may give rise to different methods. As the present work's focus is the development of conforming methods on polytopic meshes, we prefer to keep the presentation simple and consider recovery operators into conforming element-wise polynomials of the same order ($r = s$) but, crucially, posed on different meshes. For an investigation of the case $r \neq s$ on standard element shapes, we refer to [21].

4 Design concepts for recovered finite element methods

Equipped with a finite element space framework and the concept of recovery operators, we can now describe some general principles in the design of recovered finite element methods on polytopic meshes.

To this end, we consider a generic conforming Galerkin finite element method for the problem (1), (3), which is applicable on a *simplicial* mesh, say $\tilde{\mathcal{T}}$, with respective finite element space $V_h \subset V$, reading: find $\tilde{u}_h \in \tilde{V}_h$, such that

$$a_h(\tilde{u}_h, \tilde{v}_h) = \ell_h(\tilde{v}_h), \quad \text{for all } \tilde{v}_h \in \tilde{V}_h; \quad (9)$$

an example of a stable such conforming method is the streamline upwind Petrov-Galerkin approach presented and analysed in [26].

Suppose also that the bilinear form a_h is coercive in \tilde{V}_h with respect to an “energy”-like norm $\|\cdot\|_a$, i.e., for all $w \in \tilde{V}_h$, there exists a $C_{\text{coer}} > 0$, such that

$$C_{\text{coer}} \|w\|_a^2 \leq a_h(w, w), \quad (10)$$

and that a is also continuous in $V \times \tilde{V}_h$, in the sense that for all $z \in V$ and all $w \in \tilde{V}_h$, there exists a constant $C_{\text{cont}} > 0$, such that

$$|a_h(z, w)| \leq C_{\text{cont}} \|z\|_a \|w\|_a, \quad (11)$$

for some norm $\|\cdot\|_a$, possibly different to $\|\cdot\|_a$. Of course, this is relevant if $\|\cdot\|_a$ is stronger than $\|\cdot\|_a$ for, otherwise, we can replace $\|\cdot\|_a$ by $\|\cdot\|_a$ throughout this section. Hence, without any loss of generality in this context, we henceforth assume $\|w\|_a \leq C \|\tilde{w}\|_a$ for all $w \in V$ with $C > 0$ independent of w .

A corresponding *recovered finite element method* (R-FEM) can be, then, defined on a *polytopic* mesh \mathcal{T} , (with respective finite element space V_h^r), which admits a subtriangulation $\tilde{\mathcal{T}}$, (and a respective space \tilde{V}_h^r), as discussed in detail in Section 3 with the help of a recovery operator $\mathcal{E} : V_h^r \rightarrow V \cap \tilde{V}_h^r$. To this end, we consider the R-FEM: find $u_h \in V_h^r$ (and, consequently, also $\mathcal{E}(u_h) \in V \cap \tilde{V}_h^r$) such that

$$a_h(\mathcal{E}(u_h), \mathcal{E}(v_h)) + s_h(u_h, v_h) = \ell_h(\mathcal{E}(v_h)), \quad \text{for all } v_h \in V_h^r, \quad (12)$$

for $s_h : (\tilde{V}_h^r \cap \prod_{T \in \mathcal{T}} H^1(T)) \times (\tilde{V}_h^r \cap \prod_{T \in \mathcal{T}} H^1(T)) \rightarrow \mathbb{R}$ a symmetric bilinear form, henceforth referred to as the *stabilization*, whose role is to remove the possible rank-deficiency due to the use of a recovery operator. Note that $V_h^r \subset (\tilde{V}_h^r \cap \prod_{T \in \mathcal{T}} H^1(T))$.

An immediate choice for stabilization can be:

$$s_h(w_h, v_h) = C \int_{\Omega} \mathbf{h}^m (w_h - \mathcal{E}(w_h)) (v_h - \mathcal{E}(v_h)) \, dx, \quad (13)$$

for $v_h \in V_h^r$, with $m \in \mathbb{R}$ a real number, to be determined by the error analysis in each case. When \mathcal{E} is as in Lemma 3.1, (7) allows also to consider the alternative stabilization

$$s_h(w_h, v_h) = C \int_{\Gamma_{\text{int}}} \mathbf{h}^{m-1} [w_h] \cdot [v_h] \, ds. \quad (14)$$

To keep the discussion general at this point, we avoid prescribing a specific stabilization, and we prefer to make a structural assumption on s_h instead.

Assumption 4.1 *The stabilization bilinear form satisfies*

$$s_h(w_h, v_h) \leq C_{\text{stab}} (s_h(w_h, w_h))^{1/2} (s_h(v_h, v_h))^{1/2} \quad \text{for all } w_h, v_h \in V_h^r,$$

for some constant $C_{\text{stab}} > 0$ independent of w_h, v_h and of \mathbf{h} .

Now given the PDE problem (1), (3) in weak form, reading: find $u \in V$ such that

$$a(u, v) = \ell(v) \quad \text{for all } v \in V. \quad (15)$$

We can now show the following best approximation result:

Lemma 4.2 *Let $u \in V$ satisfy (15) and, for $r \geq 1$, suppose $u_h \in V_h^r$ is the R-FEM approximation with a stabilisation term satisfying Assumption 4.1 then we have*

$$\begin{aligned} \frac{1}{2} \|u - \mathcal{E}(u_h)\|_a^2 + C_{\text{coer}}^{-1} s_h(u_h, u_h) &\leq \inf_{v_h \in V_h^r} \left(\left(1 + 2 \frac{C_{\text{cont}}^2}{C_{\text{coer}}^2} \right) \|u - \mathcal{E}(v_h)\|_a^2 + \frac{C_{\text{stab}}^2}{C_{\text{coer}}^2} s_h(v_h, v_h) \right) \\ &\quad + \text{INC}(u), \end{aligned} \quad (16)$$

where

$$\text{INC}(u) := \frac{2}{C_{\text{coer}}^2} \sup_{0 \neq \tilde{w}_h \in \mathcal{E}(V_h^r)} \left(\frac{|\ell_h(\tilde{w}_h) - \ell(\tilde{w}_h)|}{\|\tilde{w}_h\|_a} + \frac{|a(u, \tilde{w}_h) - a_h(u, \tilde{w}_h)|}{\|\tilde{w}_h\|_a} \right)^2,$$

and $C_{\text{coer}}, C_{\text{cont}}$ are the coercivity and continuity constants defined in (10), (11) independent of u, u_h, h and of \mathcal{E} .

Proof. With $\xi := \mathcal{E}(v_h - u_h) \in \tilde{V}_h^r \cap V \equiv \tilde{V}_h$, coercivity (10) implies

$$C_{coer} \|\xi\|_a^2 + s_h(u_h, u_h) \leq a_h(\xi, \xi) + s_h(u_h, u_h),$$

and hence, in view of (12), (15) adding and subtracting appropriate terms yields

$$\begin{aligned} C_{coer} \|\xi\|_a^2 + s_h(u_h, u_h) &\leq a_h(\mathcal{E}(v_h), \xi) - \ell_h(\xi) + s_h(u_h, v_h) \\ &\leq a_h(\mathcal{E}(v_h) - u, \xi) + s_h(u_h, v_h) + \ell(\xi) - \ell_h(\xi) + a_h(u, \xi) - a(u, \xi). \end{aligned}$$

Making use of the continuity (11) of a_h along with and Assumption 4.1 we see

$$\begin{aligned} \|\xi\|_a^2 + \frac{1}{C_{coer}} s_h(u_h, u_h) &\leq \frac{C_{cont}}{C_{coer}} \|u - \mathcal{E}(v_h)\|_a \|\xi\|_a + \frac{C_{stab}}{C_{coer}} (s_h(u_h, u_h))^{1/2} (s_h(v_h, v_h))^{1/2} \\ &\quad + \frac{1}{C_{coer}} (\ell(\xi) - \ell_h(\xi) + a_h(u, \xi) - a(u, \xi)). \end{aligned}$$

Finally, invoking Hölders inequality in standard fashion shows the abstract bound

$$\|\xi\|_a^2 + \frac{1}{C_{coer}} s_h(u_h, u_h) \leq 2 \frac{C_{cont}^2}{C_{coer}^2} \|u - \mathcal{E}(v_h)\|_a^2 + \frac{C_{stab}^2}{C_{coer}} s_h(v_h, v_h) + \text{INC}(u).$$

The result follows by the triangle inequality and noticing that v_h was arbitrary. \square

To arrive at an a priori error bound, we make the following (rather mild and immediately satisfiable by all the scenarios we have in mind) additional set of assumptions.

Assumption 4.3 *There exists a “broken” version of $\|\cdot\|_a$, say $\|\cdot\|_{a,\mathcal{T}}$, elementwise with respect to \mathcal{T} , for which we have $\|w\|_{a,\mathcal{T}} = \|w\|_a$ whenever $w \in \tilde{V}_h^r \cap V$. Moreover, for $C_{ker}, c_{ker} > 0$ representing constants independent of \mathbf{h} and of w the stabilization s_h satisfies*

$$c_{ker} s_h(w, w) \leq \|w - \mathcal{E}(w)\|_{a,\mathcal{T}}^2 \leq C_{ker} s_h(w, w) \quad \text{for all } w \in \tilde{V}_h^r \cap \prod_{T \in \mathcal{T}} H^1(T).$$

That is, this equivalence holds for all elementwise polynomials defined over the simplicial sub-mesh \mathcal{T} that are continuous within in each element T of the related polytopic mesh.

Finally, assume that there exists a “broken” version of $\|\cdot\|_a$, denoted by $\|\cdot\|_{a,\mathcal{T}}$, elementwise with respect to \mathcal{T} , for which we have:

1. $\|w\|_{a,\mathcal{T}} = \|w\|_a$ whenever $w \in \tilde{V}_h^r \cap V$ and
2. $\|w\|_{a,\mathcal{T}} \leq C \|w\|_{a,\mathcal{T}}$ for all $w \in (\tilde{V}_h^r \cap \prod_{T \in \mathcal{T}} H^1(T))$ for some $C > 0$ independent of w and \mathbf{h} .

Theorem 4.4 *Assume that the recovery operator \mathcal{E} in the definition of R-FEM (12) is such that $\mathcal{E}(v) = v$ for all $v \in \tilde{V}_h^r \cap V$ and, also, that it is stable with respect to the $\|\cdot\|_{a,\mathcal{T}}$ -norm, viz.,*

$$\|\mathcal{E}(w)\|_a \leq C \|w\|_{a,\mathcal{T}} \quad \forall w \in V_h^r.$$

Assume that the exact solution satisfies $u \in \prod_{T \in \mathcal{T}} H^k(T)$, for some $k \geq 2$, and that any inconsistency of the Galerkin method posed on simplices (9) is of optimal order, viz.,

$$\text{INC}(u) \leq C \sum_{T \in \tilde{\mathcal{T}}} \mathbf{h}^{2s} |u|_{s,T}^2,$$

for $1 \leq s = \min\{k, r\}$, with constant $C > 0$, independent of u and \mathbf{h} . Then, we have the bound

$$\|u - \mathcal{E}(u_h)\|_a^2 + s_h(u_h, u_h) \leq C \sum_{T \in \tilde{\mathcal{T}}} \mathbf{h}^{2s} |u|_{s,T}^2. \quad (17)$$

Proof. The triangle inequality, Assumption 4.3 along with the optimality of the inconsistency terms imply

$$\|u - \mathcal{E}(u_h)\|_a^2 + s_h(u_h, u_h) \leq C \|u - \Pi u\|_{a,\mathcal{T}}^2 + C s_h(\Pi u, \Pi u) + C \sum_{T \in \tilde{\mathcal{T}}} \mathbf{h}^{2s} |u|_{s,T}^2, \quad (18)$$

with $\Pi : L^2(\Omega) \rightarrow V_h^r$ denoting the orthogonal L^2 -projection operator onto the polytopic finite element space V_h^r . Let also $\tilde{\Pi} : L^2(\Omega) \rightarrow \tilde{V}_h^r \cap V$ be the respective orthogonal L^2 -projection onto the conforming finite element space of the subtriangulation $\tilde{\mathcal{T}}$. The above mesh assumptions on \mathcal{T} and on $\tilde{\mathcal{T}}$ ensure that Π and $\tilde{\Pi}$ admit optimal approximation properties.

From hypothesis, we have $\mathcal{E}(\tilde{\Pi}u) = \tilde{\Pi}u$. From Assumption 4.3, it then follows $s_h(\tilde{\Pi}u, \tilde{\Pi}u) = 0$. Now, from Assumption 4.1, we then also have

$$s_h(\tilde{\Pi}u, v) = s_h(v, \tilde{\Pi}u) = 0 \text{ for any } v \in \tilde{V}_h^r \cap \prod_{T \in \mathcal{T}} H^1(T).$$

Using this, together with Assumption 4.3 and the stability of the recovery operator, we have, respectively,

$$\begin{aligned} s_h(\Pi u, \Pi u) &= s_h(\tilde{\Pi}u - \Pi u, \tilde{\Pi}u - \Pi u) \\ &\leq c_{ker}^{-1} \|\tilde{\Pi}u - \Pi u - \mathcal{E}(\tilde{\Pi}u - \Pi u)\|_{a,\mathcal{T}}^2 \\ &\leq C (\|\tilde{\Pi}u - \Pi u\|_{a,\mathcal{T}}^2 + \|\tilde{\Pi}u - \Pi u\|_{a,\mathcal{T}}^2) \\ &\leq C \|\tilde{\Pi}u - \Pi u\|_{a,\mathcal{T}}^2 \\ &\leq C (\|u - \tilde{\Pi}u\|_{a,\mathcal{T}} + \|u - \Pi u\|_{a,\mathcal{T}})^2. \end{aligned}$$

The result now follows by appealing to the optimal approximation properties of Π and $\tilde{\Pi}$. \square

Corollary 4.5 *With the assumptions of Theorem 4.4, we also have the following bound:*

$$\|u - u_h\|_{a,\mathcal{T}}^2 + s_h(u_h, u_h) \leq C \sum_{T \in \tilde{\mathcal{T}}} \mathbf{h}^{2s} |u|_{s,T}^2, \quad (19)$$

for $1 \leq s = \min\{k, r\}$, with C positive constant, independent of u and of \mathbf{h} .

Proof. The triangle inequality implies

$$\|u - u_h\|_{a,\mathcal{T}} \leq \|u - \mathcal{E}(u_h)\|_a + \|\mathcal{E}(u_h) - u_h\|_{a,\mathcal{T}}.$$

Using, now, Assumption 4.3 we have

$$\|\mathcal{E}(u_h) - u_h\|_{a,\mathcal{T}} \leq C_{ker} s_h(u_h, u_h),$$

the result then follows. \square

5 An alternative recovered finite element method

To highlight further the potential of the proposed R-FEM framework applied to both standard/simplicial/box and, in general, polytopic meshes, we present an alternative R-FEM. This method is motivated by the desire to have a conforming approximation for the second order part of the differential operator and an upwinded discontinuous Galerkin discretization of the first order terms in (1). The developments below also showcase an R-FEM error analysis using inf-sup stability rather than coercivity results.

For sake of the simplicity of exposition, we assume that each entries of the diffusion tensor a are constant on each element $T \in \mathcal{T}$, i.e.,

$$a \in [V_h^0]_{\text{sym}}^{d \times d}. \quad (20)$$

Additionally, we assume the following standard assumption on \mathbf{b} :

$$\mathbf{b} \cdot \nabla_h \xi \in V_h^r \quad \forall \xi \in V_h^r. \quad (21)$$

cf. [25, 7]. For given operator (6), the new *recovered finite element method* reads: find $u_h \in V_h^r$ such that

$$B(u_h, v_h) = \ell(v_h), \quad \text{for all } v_h \in V_h^r, \quad (22)$$

where

$$\begin{aligned} B(u_h, v_h) := & \int_{\Omega} \left(a \nabla \mathcal{E}(u_h) \cdot \nabla \mathcal{E}(v_h) + \mathbf{b} \cdot \nabla_h u_h \mathcal{E}(v_h) + c \mathcal{E}(u_h) \mathcal{E}(v_h) \right) dx \\ & - \int_{\Gamma_D} \left(a \nabla \mathcal{E}(u_h) \cdot \mathbf{n} \mathcal{E}(v_h) + a \nabla \mathcal{E}(v_h) \cdot \mathbf{n} \mathcal{E}(u_h) - \sigma_D \mathcal{E}(u_h) \mathcal{E}(v_h) \right) ds \\ & - \int_{\Gamma_D^-} (\mathbf{b} \cdot \mathbf{n}) u_h \mathcal{E}(v_h) ds - \sum_{T \in \mathcal{T}} \int_{\partial_- T \setminus \partial \Omega} (\mathbf{b} \cdot \mathbf{n}) [u_h] \mathcal{E}(v_h) ds \\ & + s_h^{a,c}(u_h, v_h) + s_h^b(u_h, v_h), \end{aligned} \quad (23)$$

and

$$\begin{aligned} \ell(v_h) := & \int_{\Omega} f \mathcal{E}(v_h) dx - \int_{\Gamma_D} g_D \left(a \nabla \mathcal{E}(v_h) \cdot \mathbf{n} - \sigma_D \mathcal{E}(v_h) \right) ds + \int_{\Gamma_N} g_N \mathcal{E}(v_h) ds \\ & - \int_{\Gamma_D^-} (\mathbf{b} \cdot \mathbf{n}) g_D \mathcal{E}(v_h) ds, \end{aligned}$$

with $s_h^m(\cdot, \cdot) : V_h^r \times V_h^r \rightarrow \mathbb{R}$, $m \in \{a, c, b\}$ denoting symmetric bilinear forms, henceforth referred to as *stabilisations*, and $\sigma_D : \Gamma_D \rightarrow \mathbb{R}$ a positive penalty function defined precisely below that weakly enforces the Dirichlet boundary conditions.

This motivates the following choice for the elliptic stabilisation bilinear form:

$$s_h^{a,c}(u_h, v_h) := \int_{\Gamma_{\text{int}}} \sigma_{a,c} [u_h] \cdot [v_h] ds, \quad (24)$$

for some non-negative function $\sigma_{a,c} : \Gamma_{\text{int}} \rightarrow \mathbb{R}$, that will also be defined below.

To ensure that sufficient numerical diffusion is included in the proposed method for the case of small or vanishing diffusion tensor a , we select

$$s_h^b(u_h, v_h) := \int_{\Gamma_{\text{int}}} \left(\sigma_{b,1} [u_h] \cdot [v_h] + \sigma_{b,2} [\mathbf{h}(\mathbf{b} \cdot \nabla u_h)] \cdot [\mathbf{h}(\mathbf{b} \cdot \nabla v_h)] \right) ds, \quad (25)$$

for non-negative functions $\sigma_{b,1}, \sigma_{b,2} : \Gamma_{\text{int}} \rightarrow \mathbb{R}$, to be selected below. We note that (25) follows the spirit of the, so-called, continuous interior penalty stabilisation procedure due to Douglas and Dupont [17] and to Burman and Hansbo [5]. Crucially, however, the trial and test functions u_h and v_h in the present R-FEM context are discontinuous, cf., [4] also. The inconsistency introduced by the streamline derivative jump term in (25) will be dealt with in the a priori error analysis below.

Some remarks on the method are in order. To accommodate for the potentially locally changing nature of the differential operator, we have opted for weak imposition of essential boundary conditions, following the classical ideas from [28, 32]. For the case of elliptic problems, strong imposition of essential boundary conditions in the spirit of [21] is by all means possible also. We note, however, that since essential boundary values are known the above is actually a conforming method for $\mathcal{E}(u_h)$.

Also, we have opted for a, to the best of our knowledge, new method for the discretisation of the first order term. This is to highlight the flexibility of RFEM in incorporating different discretisations of various terms of the differential operator. More importantly, since in the absence of diffusion, the exact solution u may exhibit jump discontinuities across characteristic surfaces, we prefer not to recover u_h in the discretisation of the first order term. We stress that more classical choices, such as streamline diffusion-type and/or continuous interior penalty-type treatment of the first order term are by all means possible. Indeed, certain such choices coincide with the standard/classical conforming finite element versions for $\mathcal{E}(u_h)$ when applied to standard triangular meshes (cf., the discussion in Section 3 of [21]).

We also remark on the assumptions on the diffusion tensor (20) and convection field (21). The above RFEM method (22) can be easily extended to general positive semi-definite diffusion $a \in [L^\infty(\Omega)]_{\text{sym}}^{d \times d}$ following the inconsistent formulation introduced in [20]. For the general convection field \mathbf{b} , we would need to modify (25) by setting

$$s_h^b(u_h, v_h) = \int_{\Gamma_{\text{int}}} \left(\sigma_{b,1}[u_h] \cdot [v_h] + \sigma_{b,2}[\mathbf{h}\Pi(\mathbf{b} \cdot \nabla u_h)] \cdot [\mathbf{h}\Pi(\mathbf{b} \cdot \nabla v_h)] \right) ds, \quad (26)$$

which will make the stability proof and error analysis more complicated. We refrain from doing this here to focus on the key ideas.

6 A priori error analysis

We dedicate this section to the analysis of the method introduced in Section 5. The main ingredient to this is an inf-sup condition over suitable norms. We let $\alpha, \beta, \gamma : \Omega \rightarrow \mathbb{R}$ such that

$$\alpha|_T := |\sqrt{a}|_2^2|_T, \quad \beta|_T := \|\mathbf{b}\|_{L^\infty(T)}, \quad \gamma|_T := \|c\|_{L^\infty(T)}, \quad (27)$$

over each element $T \in \mathcal{T}$. We define the stabilisation parameter

$$\sigma_D := C_\sigma \alpha r^2 / \mathbf{h}, \quad \tilde{\sigma}_D|_T := \max_{e \subset \partial T} \sigma_D|_e. \quad (28)$$

Now, for $w \in V_h^r$, we define the norms

$$\|w\|_b := \left(\|\sqrt{c_0}w\|^2 + \frac{1}{2} \left(\|\sqrt{|\mathbf{b} \cdot \mathbf{n}|}[w]\|_{\Gamma_{\text{int}}}^2 + \|\sqrt{|\mathbf{b} \cdot \mathbf{n}|}w\|_{\Gamma_D^-}^2 + \|\sqrt{|\mathbf{b} \cdot \mathbf{n}|}w\|_{\Gamma_N^+}^2 \right) \right)^{1/2},$$

and

$$\|w\| := \left(\|\sqrt{a}\nabla \mathcal{E}(w)\|^2 + \|\sqrt{\sigma_D}\mathcal{E}(w)\|_{\Gamma_D}^2 + \|w\|_b^2 + s_h^{a,c}(w, w) + s_h^b(w, w) \right)^{1/2}.$$

We also define the ‘streamline-diffusion’ norm

$$\|w\|_s := (\|w\|^2 + \|\sqrt{\delta\boldsymbol{\lambda}}(\mathbf{b} \cdot \nabla_h w)\|^2)^{1/2},$$

where $\delta > 0$, to be chosen precisely below, and

$$\boldsymbol{\lambda} := \min\{\beta^{-1}, \tilde{\sigma}_D^{-1}\}\mathbf{h}, \quad (29)$$

We are now in a position to show the following inf-sup condition for the R-FEM method (22). In the proofs of the results in this section, we are particularly interested in the dependence of the resulting bounds on the mesh-Péclet number Pe_h , the mesh-size \mathbf{h} and polynomial degree r . We aim, therefore, to track constants and their dependence explicitly.

Theorem 6.1 (Inf-Sup Condition) *Let $a \in [L^\infty(\Omega)]_{sym}^{d \times d}$ satisfy Assumption (20) and $\mathbf{b} \in W^{1,\infty}(\Omega)^d$ satisfy Assumption (21). Assume that the mesh is such that each element face in the mesh is either completely inflow or outflow or characteristic. Suppose also that the penalisation parameters $\sigma_{a,c}, \sigma_{b,1}$ and $\sigma_{b,2}$ are chosen large enough to satisfy (36), δ is chosen to satisfy (37) and the boundary stabilisation constant $C_\sigma > 0$ is sufficiently large. Then, we have*

$$\inf_{0 \neq w_h \in V_h^r} \sup_{0 \neq v_h \in V_h^r} \frac{B(w_h, v_h)}{\|w_h\|_s \|v_h\|_s} \geq \Lambda, \quad (30)$$

where $\Lambda > 0$ is independent of $\boldsymbol{\lambda}$, \mathbf{h} and of the mesh-Péclet number $Pe_h := \beta\mathbf{h}/\alpha$.

Proof. As usual, the proof consists of two steps: 1) for each $w_h \in V_h^r$, we find a $v_h(w_h) \equiv v_h \in V_h^r$ such that $B(w_h, v_h) \geq C\|w_h\|_s^2$, and, 2) we show that this v_h satisfies the bound $\|v_h\|_s \leq C\|w_h\|_s$, thereby inferring the result.

To that end, fix $w_h \in V_h^r$ and set $v_h = w_h + \delta w_h^b$, where we will use the shorthand $w_h^b := \boldsymbol{\lambda}(\mathbf{b} \cdot \nabla_h w_h)$ for brevity for some $\delta \in \mathbb{R}$ is to be chosen. Then, integration by parts and working as in the proof of [24, Lemma 2.4], as well as making use of standard inverse estimates, give

$$\begin{aligned} B(w_h, w_h) &\geq \frac{1}{2}\|w_h\|^2 + \int_{\Omega} \mathbf{b} \cdot \nabla_h w_h (\mathcal{E}(w_h) - w_h) dx + \int_{\Omega} c(\mathcal{E}(w_h)^2 - w_h^2) dx \\ &\quad - \int_{\Gamma_D^-} (\mathbf{b} \cdot \mathbf{n}) w_h (\mathcal{E}(w_h) - w_h) ds - \sum_{T \in \mathcal{T}} \int_{\partial_- T \setminus \partial\Omega} (\mathbf{b} \cdot \mathbf{n}) [w_h] (\mathcal{E}(w_h) - w_h) ds \\ &=: \frac{1}{2}\|w_h\|^2 + \text{I} + \text{II} + \text{III} + \text{IV}. \end{aligned} \quad (31)$$

Using Lemma 3.1, Young’s inequality and (29), we have

$$\text{I} \leq \frac{1}{4}\|\sqrt{\delta\boldsymbol{\lambda}}\mathbf{b} \cdot \nabla_h w_h\|^2 + C(r)\|\delta^{-1/2}\beta^{1/2}[w_h]\|_{\Gamma_{\text{int}}}^2.$$

and

$$\begin{aligned} \text{II} &= \int_{\Omega} c(\mathcal{E}(w_h) - w_h)^2 + 2cw_h(\mathcal{E}(w_h) - w_h) dx \\ &\leq C(r)\|\sqrt{\gamma\mathbf{h}}[w_h]\|_{\Gamma_{\text{int}}}^2 + \frac{1}{4}\|\sqrt{c_0}w_h\|^2 + C(r)\|\sqrt{\gamma/\gamma_0}\sqrt{\gamma\mathbf{h}}[w_h]\|_{\Gamma_{\text{int}}}^2 \\ &\leq \frac{1}{4}\|\sqrt{c_0}w_h\|^2 + C(r)\|(1 + \sqrt{\gamma/\gamma_0})\sqrt{\gamma\mathbf{h}}[w_h]\|_{\Gamma_{\text{int}}}^2, \end{aligned}$$

with γ_0 a local min of c_0 . Finally, again, using Lemma 3.1 and Young’s inequality, we also have

$$\text{III} + \text{IV} \leq \frac{1}{8}\|\sqrt{|\mathbf{b} \cdot \mathbf{n}|}w_h\|_{\Gamma_D^-}^2 + \frac{1}{8}\|\sqrt{|\mathbf{b} \cdot \mathbf{n}|}[w_h]\|_{\Gamma_{\text{int}}}^2 + C(r)\|\sqrt{\beta}[w_h]\|_{\Gamma_{\text{int}}}^2.$$

Substituting the above bounds into (31), we arrive at

$$\begin{aligned}
B(w_h, w_h) &\geq \frac{1}{2} \|w_h\|^2 - \frac{1}{4} \|\sqrt{c_0} w_h\|^2 - C(r) \|(1 + \sqrt{\gamma/\gamma_0}) \sqrt{\gamma} \mathbf{h}[w_h]\|_{\Gamma_{\text{int}}}^2 \\
&\quad - \frac{1}{8} \|\sqrt{|\mathbf{b} \cdot \mathbf{n}|} w_h\|_{\Gamma_{\text{D}}}^2 - \frac{1}{8} \|\sqrt{|\mathbf{b} \cdot \mathbf{n}|} [w_h]\|_{\Gamma_{\text{int}}}^2 - \frac{1}{4} \|\sqrt{\delta} \bar{\lambda} \mathbf{b} \cdot \nabla_h w_h\|^2 \\
&\quad - C(r) \|(\sqrt{\beta} + \delta^{-1/2} \sqrt{\beta}) [w_h]\|_{\Gamma_{\text{int}}}^2.
\end{aligned} \tag{32}$$

Working as before, we also have

$$\begin{aligned}
B(w_h, \delta w_h^b) &\geq -\frac{1}{4} \|w_h\| - \|\sqrt{a} \nabla \mathcal{E}(\delta w_h^b)\|^2 \\
&\quad + \|\sqrt{\delta} \bar{\lambda} \mathbf{b} \cdot \nabla_h w_h\|^2 + \int_{\Omega} \mathbf{b} \cdot \nabla_h w_h (\mathcal{E}(\delta w_h^b) - \delta w_h^b) dx \\
&\quad - 2 \|\sqrt{\sigma_{\text{D}}} \mathcal{E}(\delta w_h^b)\|_{\Gamma_{\text{D}}}^2 - 8 \|\sigma_{\text{D}}^{-1/2} a \nabla \mathcal{E}(\delta w_h^b)\|_{\Gamma_{\text{D}}}^2 \\
&\quad - 2 \|\sqrt{|\mathbf{b} \cdot \mathbf{n}|} \mathcal{E}(\delta w_h^b)\|_{\Gamma_{\text{D}}}^2 - 2 \|\sqrt{|\mathbf{b} \cdot \mathbf{n}|} \mathcal{E}(\delta w_h^b)\|_{\Gamma_{\text{int}}}^2 \\
&\quad - \|\sqrt{\sigma_{a,c}} [\delta w_h^b]\|_{\Gamma_{\text{int}}}^2 - \|\sqrt{\sigma_{b,1}} [\delta w_h^b]\|_{\Gamma_{\text{int}}}^2 - \|\sqrt{\sigma_{b,2}} [\mathbf{h}(\mathbf{b} \cdot \nabla(\delta w_h^b))]\|_{\Gamma_{\text{int}}}^2.
\end{aligned} \tag{33}$$

We further bound each term in (33) not directly appearing in the energy norm. We have

$$\begin{aligned}
\|\sqrt{a} \nabla \mathcal{E}(\delta w_h^b)\|^2 &\leq Cr^4 \|\sqrt{\alpha} \mathbf{h}^{-1} \mathcal{E}(\delta w_h^b)\|^2 \\
&\leq Cr^4 \|\sqrt{\delta} (\sqrt{\delta} \bar{\lambda} \mathbf{b} \cdot \nabla_h w_h)\|^2 + C(r) \|[\delta \mathbf{h}(\mathbf{b} \cdot \nabla_h w_h)]\|_{\Gamma_{\text{int}}}^2,
\end{aligned} \tag{34}$$

using an inverse estimate and Lemma 3.1, respectively. Similarly,

$$\int_{\Omega} \mathbf{b} \cdot \nabla_h w_h (\mathcal{E}(\delta w_h^b) - \delta w_h^b) dx \leq \frac{1}{4} \|\sqrt{\delta} \bar{\lambda} \mathbf{b} \cdot \nabla_h w_h\|^2 + C(r) \|[\sqrt{\delta} \mathbf{h}(\mathbf{b} \cdot \nabla_h w_h)]\|_{\Gamma_{\text{int}}}^2.$$

Next, using the stability of \mathcal{E} , we deduce

$$2 \|\sqrt{\sigma_{\text{D}}} \mathcal{E}(\delta w_h^b)\|_{\Gamma_{\text{D}}}^2 \leq Cr^4 \|\sqrt{\delta} (\sqrt{\delta} \bar{\lambda} \mathbf{b} \cdot \nabla_h w_h)\|^2 + C(r) \|[\delta \mathbf{h}(\mathbf{b} \cdot \nabla_h w_h)]\|_{\Gamma_{\text{int}}}^2,$$

and, using inverse estimates along with the definition of σ_{D} ,

$$8 \|\sigma_{\text{D}}^{-1/2} a \nabla \mathcal{E}(\delta w_h^b)\|_{\Gamma_{\text{D}}}^2 \leq Cr^4 \|\sqrt{\alpha} \mathbf{h}^{-1} \mathcal{E}(\delta w_h^b)\|^2,$$

which can be further estimated as in (34). We also have

$$2 \|\sqrt{|\mathbf{b} \cdot \mathbf{n}|} \mathcal{E}(\delta w_h^b)\|_{\Gamma_{\text{D}} \cup \Gamma_{\text{int}}}^2 \leq Cr^2 \|\sqrt{\delta} (\sqrt{\delta} \bar{\lambda} \mathbf{b} \cdot \nabla_h w_h)\|^2 + C(r) \|[\delta \mathbf{h}(\mathbf{b} \cdot \nabla_h w_h)]\|_{\Gamma_{\text{int}}}^2,$$

and

$$\|\sqrt{\sigma_{b,2}} [\mathbf{h}(\mathbf{b} \cdot \nabla_h(\delta w_h^b))]\|_{\Gamma_{\text{int}}}^2 \leq Cr^6 \|\sqrt{\sigma_{b,2}/\mathbf{h}} \delta w_h^b\|^2 \leq Cr^6 \|\sqrt{\sigma_{b,2}\beta} (\sqrt{\delta} \bar{\lambda} \mathbf{b} \cdot \nabla_h w_h)\|^2.$$

Combining now the above estimates, we arrive at the bound

$$\begin{aligned}
B(w_h, v_h(w_h)) &\geq \frac{1}{4} \|w_h\|^2 + \frac{1}{2} \|\sqrt{\delta} \bar{\lambda} \mathbf{b} \cdot \nabla_h w_h\|^2 \\
&\quad - C(r) \|(\sqrt{\beta} + \sqrt{\beta} \delta^{-1/2}) [w_h]\|_{\Gamma_{\text{int}}}^2 - C(r) \|(1 + \sqrt{\gamma/\gamma_0}) \sqrt{\gamma} \mathbf{h}[w_h]\|_{\Gamma_{\text{int}}}^2 \\
&\quad - Cr^4 \|\sqrt{\delta} (1 + r^{-1} + r \sqrt{\sigma_{b,2}\beta}) (\sqrt{\delta} \bar{\lambda} \mathbf{b} \cdot \nabla_h w_h)\|^2 \\
&\quad - C(r) \|(\sqrt{\sigma_{b,1}} + 1 + \delta^{-1/2}) [\delta \mathbf{h}(\mathbf{b} \cdot \nabla_h w_h)]\|_{\Gamma_{\text{int}}}^2.
\end{aligned} \tag{35}$$

Upon selecting a global constant $\delta > 0$, small enough, we can have

$$Cr^4\delta\left(1+r^{-1}+r\sqrt{\sigma_{b,2}\beta}\right)^2 \leq \frac{1}{4} \quad \text{and} \quad \delta^2 C(r)\left(\sqrt{\sigma_{b,1}}+1+\delta^{-1/2}\right)^2 \leq \frac{\sigma_{b,2}}{8}.$$

Now, upon selecting additionally penalty parameters large enough to satisfy

$$\sigma_{b,1} \geq 8C(r)\beta(1+\delta^{-1/2})^2, \quad \sigma_{a,c} \geq 8C(r)\gamma(1+\sqrt{\gamma/\gamma_0})^2, \quad \sigma_{b,2} > 0, \quad (36)$$

we can set

$$\delta := \min\left\{\left(4Cr^4(1+r^{-1}+r\sqrt{\sigma_{b,2}\beta})^2\right)^{-1}, \left(-1+\sqrt{1+\sqrt{\sigma_{b,2}}(2\sqrt{C(r)\beta}+2^{-1/2})^{-1}}\right)^2/4\right\}. \quad (37)$$

which, in turn implies,

$$B(w_h, v_h(w_h)) \geq \frac{1}{8}\|w_h\|^2 + \frac{1}{4}\|\sqrt{\delta}\mathbf{h}(\mathbf{b} \cdot \nabla_h w_h)\|^2 \geq \frac{1}{8}\|w_h\|_s^2, \quad (38)$$

from (35) and the first step of the proof is complete.

For the second step, working as above, standard inverse estimates along with and Lemma 3.1 imply

$$\begin{aligned} \|\delta w_h^b\|^2 &\leq C(r)\|\delta\mathbf{h}(\mathbf{b} \cdot \nabla_h w_h)\|_{\Gamma_{\text{int}}}^2 + Cr^4\|\sqrt{\delta}(\sqrt{\delta}\mathbf{\lambda}\mathbf{b} \cdot \nabla_h w_h)\|^2 + \|\sqrt{c_0\delta}\mathbf{\lambda}\sqrt{\delta}\mathbf{\lambda}\mathbf{b} \cdot \nabla_h w_h\|^2 \\ &\quad + \|\sqrt{\sigma_{a,c}}[\delta w_h^b]\|_{\Gamma_{\text{int}}}^2 + Cr^2\|\sqrt{\beta\delta}\sqrt{\delta}\mathbf{\lambda}\mathbf{b} \cdot \nabla_h w_h\|_{\Gamma_{\text{int}}}^2 + \|\sqrt{\sigma_{b,1}}[\delta w_h^b]\|_{\Gamma_{\text{int}}}^2 \\ &\quad + Cr^6\|\sqrt{\sigma_{b,2}\delta}\beta\sqrt{\delta}\mathbf{\lambda}\mathbf{b} \cdot \nabla_h w_h\|^2 \end{aligned}$$

and $\|\sqrt{\delta}\mathbf{\lambda}\mathbf{b} \cdot \nabla_h \delta w_h^b\|^2 \leq Cr^4\|\delta\sqrt{\delta}\mathbf{\lambda}\mathbf{b} \cdot \nabla_h w_h\|^2$. The above assumptions on δ , $\sigma_{a,c}$, $\sigma_{b,1}$, $\sigma_{b,2}$, finally imply

$$\|v_h\|_s \leq \|w_h\|_s + \|\delta w_h^b\|_s \leq C(r)(\|w_h\| + \|\sqrt{\delta}\mathbf{h}(\mathbf{b} \cdot \nabla_h w_h)\|) = C(r)\|w_h\|_s, \quad (39)$$

thereby completing the proof of the second step also. \square

Remark 6.2 *It is possible to modify the above proof by introducing a locally variable δ aiming to achieve stronger streamline-diffusion stabilization effect at the expense of mild assumptions on the local variation of δ in the computational domain, see [18] for a similar argument in a completely different context. In particular, using the elementary identity $[\delta w_h^b] = [\delta]\{w_h^b\} + \{\delta\}[w_h^b]$ valid on every face $e \subset \Gamma_{\text{int}}$, provided that $\|[\delta]\|_{L^\infty(e)}/\|\delta\|_{L^\infty(e)} \ll 1$, one can incorporate $\{w_h^b\}$ into the stabilization term $\|\sqrt{\delta}\mathbf{\lambda}\mathbf{b} \cdot \nabla_h w_h\|$.*

Proposition 6.3 (Galerkin orthogonality) *Let $u \in V$ be the solution of (1), (3). Suppose also that $u_h \in V_h^r$ is the R-FEM solution of (22) and set $e := u - \mathcal{E}(u_h)$ for brevity. Then, for all $v_h \in V_h^r$ we have:*

$$\begin{aligned} &\int_{\Omega} \left(a \nabla e \cdot \nabla \mathcal{E}(v_h) + \mathbf{b} \cdot \nabla_h (u - u_h) \mathcal{E}(v_h) + ce \mathcal{E}(v_h) \right) dx \\ &\quad - \int_{\Gamma_D} \left(a \nabla e \cdot \mathbf{n} \mathcal{E}(v_h) + a \nabla \mathcal{E}(v_h) \cdot \mathbf{n} e - \sigma_D e \mathcal{E}(v_h) \right) ds \\ &\quad - \int_{\Gamma_D^-} (\mathbf{b} \cdot \mathbf{n}) (u - u_h) \mathcal{E}(v_h) ds - \sum_{T \in \mathcal{T}} \int_{\partial_- T \setminus \partial \Omega} (\mathbf{b} \cdot \mathbf{n}) [u - u_h] \mathcal{E}(v_h) ds \\ &\quad + s_h^{a,c}(u - u_h, v_h) + s_h^b(u - u_h, v_h) = 0. \end{aligned} \quad (40)$$

Proof. To begin, from (1), (3), the consistency of the method yields

$$\begin{aligned} \int_{\Omega} a \nabla u \cdot \nabla \mathcal{E}(v_h) + \mathbf{b} \cdot \nabla u \mathcal{E}(v_h) + cu \mathcal{E}(v_h) dx - \int_{\Gamma_D} a \nabla u \cdot \mathbf{n} \mathcal{E}(v_h) ds \\ = \int_{\Omega} f \mathcal{E}(v_h) dx + \int_{\Gamma_N} g_N \mathcal{E}(v_h) ds \quad \forall v_h \in V_h^r. \end{aligned} \quad (41)$$

Noting that $\mathbf{n}^T a \mathbf{n} = 0$ implies $\mathbf{n}^T a = \mathbf{0}^T$ for a satisfying (2). Moreover, the regularity of u [29] allows to also conclude

$$s_h^{a,c}(u, v_h) = s_h^b(u, v_h) = 0 \text{ for } v_h \in V_h^r,$$

Subtracting now (22) from (41) already yields the result. \square

Lemma 6.4 *Suppose the assumptions of Theorem 6.1 hold and let u and u_h satisfy the assumptions of Proposition 6.3. In addition, let $\Pi : L^2(\Omega) \rightarrow V_h^r$ denote the orthogonal L^2 -projection operator onto the polytopic finite element space V_h^r . Upon considering the splitting $u - u_h = (u - \Pi u) - (u_h - \Pi u) =: \eta - \xi$, we have*

$$|B(\xi, v_h)| \leq F(\eta) \|v_h\|_s, \quad (42)$$

where

$$\begin{aligned} F(\eta)^2 = & 2\|\sqrt{a} \nabla(u - \mathcal{E}(\Pi u))\|^2 + 8C(r)/\sigma_{b,1} \|\sqrt{\mathbf{h} \mathbf{b}} \cdot \nabla_h \eta\|^2 + 8C(r)\beta/\sigma_{b,1} \|\sqrt{|\mathbf{b} \cdot \mathbf{n}|} \eta\|_{\Gamma_D^-}^2 \\ & + 8C(r)\beta/\sigma_{b,1} \|\sqrt{|\mathbf{b} \cdot \mathbf{n}|} [\eta]\|_{\Gamma_{\text{int}}}^2 + 2\|\sqrt{|\mathbf{b} \cdot \mathbf{n}|} \eta\|_{\Gamma_N^+}^2 + 2\|\sqrt{|\mathbf{b} \cdot \mathbf{n}|} \eta^-\|_{\Gamma_{\text{int}}}^2 \\ & + (2\|\mathbf{b}\|_{W^{1,\infty}(\Omega)}^2/\gamma_0^2) \|\sqrt{c_0} \eta\|^2 + (1 + 2\gamma^2/\gamma_0 + 8\gamma^2 C(r) \mathbf{h}/\sigma_{b,1}) \|u - \mathcal{E}(\Pi u)\|^2 \\ & + 2\|a \nabla(u - \mathcal{E}(\Pi u)) \cdot \mathbf{n} \sigma_D^{-1/2}\|_{\Gamma_D}^2 + 2C(r) \|\sqrt{\sigma_D}(u - \mathcal{E}(\Pi u))\|_{\Gamma_D}^2 \\ & + 2s_h^{a,c}(\eta, \eta) + 2s_h^b(\eta, \eta). \end{aligned}$$

Proof. Galerkin orthogonality (40), for any $v_h \in V_h^r$, gives

$$\begin{aligned} \int_{\Omega} \left(a \nabla(u - \mathcal{E}(\Pi u)) \cdot \nabla \mathcal{E}(v_h) + \mathbf{b} \cdot \nabla_h \eta \mathcal{E}(v_h) + c(u - \mathcal{E}(\Pi u)) \mathcal{E}(v_h) \right) dx \\ - \int_{\Gamma_D} \left(a \nabla(u - \mathcal{E}(\Pi u)) \cdot \mathbf{n} \mathcal{E}(v_h) + a \nabla \mathcal{E}(v_h) \cdot \mathbf{n} (u - \mathcal{E}(\Pi u)) - \sigma_D(u - \mathcal{E}(\Pi u)) \mathcal{E}(v_h) \right) ds \\ - \int_{\Gamma_D^-} (\mathbf{b} \cdot \mathbf{n}) \eta \mathcal{E}(v_h) ds - \sum_{T \in \mathcal{T}} \int_{\partial_- T \setminus \partial \Omega} (\mathbf{b} \cdot \mathbf{n}) [\eta] \mathcal{E}(v_h) ds + s_h^{a,c}(\eta, v_h) + s_h^b(\eta, v_h) \\ = \int_{\Omega} \left(a \nabla \mathcal{E}(\xi) \cdot \nabla \mathcal{E}(v_h) + \mathbf{b} \cdot \nabla_h \xi \mathcal{E}(v_h) + c \mathcal{E}(\xi) \mathcal{E}(v_h) \right) dx \\ - \int_{\Gamma_D} \left(a \nabla \mathcal{E}(\xi) \cdot \mathbf{n} \mathcal{E}(v_h) + a \nabla \mathcal{E}(v_h) \cdot \mathbf{n} \mathcal{E}(\xi) - \sigma_D \mathcal{E}(\xi) \mathcal{E}(v_h) \right) ds \\ - \int_{\Gamma_D^-} (\mathbf{b} \cdot \mathbf{n}) \xi \mathcal{E}(v_h) ds - \sum_{T \in \mathcal{T}} \int_{\partial_- T \setminus \partial \Omega} (\mathbf{b} \cdot \mathbf{n}) [\xi] \mathcal{E}(v_h) ds + s_h^{a,c}(\xi, v_h) + s_h^b(\xi, v_h) \end{aligned} \quad (43)$$

Now examining the terms appearing on the left hand side of (43) involving \mathbf{b} we see that

$$\begin{aligned}
& \int_{\Omega} \mathbf{b} \cdot \nabla_h \eta \mathcal{E}(v_h) dx - \int_{\Gamma_D^-} (\mathbf{b} \cdot \mathbf{n}) \eta \mathcal{E}(v_h) ds - \sum_{T \in \mathcal{T}} \int_{\partial_- T \setminus \partial \Omega} (\mathbf{b} \cdot \mathbf{n}) [\eta] \mathcal{E}(v_h) ds \\
&= \int_{\Omega} \mathbf{b} \cdot \nabla_h \eta (\mathcal{E}(v_h) - v_h) dx - \int_{\Gamma_D^-} (\mathbf{b} \cdot \mathbf{n}) \eta (\mathcal{E}(v_h) - v_h) ds \\
&\quad - \sum_{T \in \mathcal{T}} \int_{\partial_- T \setminus \partial \Omega} (\mathbf{b} \cdot \mathbf{n}) [\eta] (\mathcal{E}(v_h) - v_h)^+ ds - \int_{\Omega} (\mathbf{b} \cdot \nabla_h v_h + (\nabla \cdot \mathbf{b}) v_h) \eta dx \\
&\quad + \int_{\Gamma_N^+} (\mathbf{b} \cdot \mathbf{n}) \eta v_h ds + \sum_{T \in \mathcal{T}} \int_{\partial_- T \setminus \partial \Omega} (\mathbf{b} \cdot \mathbf{n}) [v_h] \eta^- ds.
\end{aligned} \tag{44}$$

Recalling that \mathbf{b} satisfies assumption (21), by using the orthogonality of Π , we immediately have $\int_{\Omega} \mathbf{b} \cdot \nabla_h v_h \eta dx = 0$. Using Lemma 3.1 and the Cauchy-Schwarz inequality, we have from (44)

$$\begin{aligned}
& \int_{\Omega} \mathbf{b} \cdot \nabla_h \eta \mathcal{E}(v_h) dx - \int_{\Gamma_D^-} (\mathbf{b} \cdot \mathbf{n}) \eta \mathcal{E}(v_h) ds - \sum_{T \in \mathcal{T}} \int_{\partial_- T \setminus \partial \Omega} (\mathbf{b} \cdot \mathbf{n}) [\eta] \mathcal{E}(v_h) ds \\
&\leq C(r) \|\sqrt{\mathbf{h}} \mathbf{b} \cdot \nabla_h \eta\| \| [v_h] \|_{\Gamma_{\text{int}}} + C(r) \sqrt{\beta} \|\sqrt{|\mathbf{b} \cdot \mathbf{n}|} \eta\|_{\Gamma_D^-} \| [v_h] \|_{\Gamma_{\text{int}}} \\
&\quad + C(r) \sqrt{\beta} \|\sqrt{|\mathbf{b} \cdot \mathbf{n}|} [\eta]\|_{\Gamma_{\text{int}}} \| [v_h] \|_{\Gamma_{\text{int}}} + \|\mathbf{b}\|_{W^{1,\infty}(\Omega)} \gamma_0^{-1} \|\sqrt{c_0} v_h\| \|\sqrt{c_0} \eta\| \\
&\quad + \|\sqrt{|\mathbf{b} \cdot \mathbf{n}|} \eta\|_{\Gamma_N^+} \|\sqrt{|\mathbf{b} \cdot \mathbf{n}|} v_h\|_{\Gamma_N^+} + \|\sqrt{|\mathbf{b} \cdot \mathbf{n}|} \eta^-\|_{\Gamma_{\text{int}}} \|\sqrt{|\mathbf{b} \cdot \mathbf{n}|} [v_h]\|_{\Gamma_{\text{int}}}.
\end{aligned} \tag{45}$$

Now making use of analogous arguments for the reaction term, the triangle inequality and Lemma 3.1, we have

$$\begin{aligned}
& \int_{\Omega} c(u - \mathcal{E}(\Pi u)) \mathcal{E}(v_h) dx \leq \gamma \|u - \mathcal{E}(\Pi u)\| \left(\|v_h\| + \|\mathcal{E}(v_h) - v_h\| \right) \\
&\leq \gamma \gamma_0^{-1/2} \|u - \mathcal{E}(\Pi u)\| \|\sqrt{c_0} v_h\| + \gamma C(r) \mathbf{h}^{1/2} \|u - \mathcal{E}(\Pi u)\| \| [v_h] \|_{\Gamma_{\text{int}}}.
\end{aligned} \tag{46}$$

As for the Dirichlet boundary, assumption (20) together with an inverse inequality, result to

$$\begin{aligned}
& \int_{\Gamma_D} a \nabla \mathcal{E}(v_h) \cdot \mathbf{n} (u - \mathcal{E}(\Pi u)) ds \leq \|\sigma_D^{-1/2} a \nabla \mathcal{E}(v_h) \cdot \mathbf{n}\|_{\Gamma_D} \|\sigma_D^{1/2} (u - \mathcal{E}(\Pi u))\|_{\Gamma_D} \\
&\leq C(r) \|\sigma_D^{1/2} (u - \mathcal{E}(\Pi u))\|_{\Gamma_D} \|\sqrt{a} \nabla \mathcal{E}(v_h)\|.
\end{aligned} \tag{47}$$

The result then follows by combining (43), (44), (45), (46), (47), thereby concluding the proof. \square

Theorem 6.5 *Suppose that the assumptions of Theorem 6.1 hold and let u and u_h satisfy the assumptions of Proposition 6.3. Suppose further that $u \in \prod_{T \in \mathcal{T}} H^k(T)$, for some $k \geq 2$. Then, we have the following a-priori error bound:*

$$\begin{aligned}
& \|\sqrt{a} \nabla e\|^2 + \|\sqrt{\sigma_D} e\|_{\Gamma_D}^2 + \|u - u_h\|_{\mathbf{b}}^2 + \|\sqrt{\delta} \mathbf{h}(\mathbf{b} \cdot \nabla_h(u - u_h))\|^2 \\
&+ s_h^{a,c}(u - u_h, u - u_h) + s_h^b(u - u_h, u - u_h) \leq C \sum_{T \in \mathcal{T}} \left(\mathcal{D}_T + \mathcal{C}_T \right) \mathbf{h}^{2l-2} |u|_{l,T}^2,
\end{aligned} \tag{48}$$

where

$$\mathcal{D}_T = \alpha + \alpha^2 \mathbf{h}^{-1} \sigma_D^{-1} + h \sigma_D, \tag{49}$$

and

$$\begin{aligned} \mathcal{C}_T = & \beta^2 \mathbf{h} / \sigma_{b,1} + \beta \mathbf{h} + (\gamma^2 / \gamma_0) \mathbf{h}^2 + (\|\mathbf{b}\|_{W^{1,\infty}(\Omega)}^2 \|c_0\|_{L^\infty(\Omega)} / \gamma_0^2) \mathbf{h}^2 + \|c_0\|_{L^\infty(\Omega)} \mathbf{h}^2 \\ & + \gamma^2 C(r) \mathbf{h}^3 / \sigma_{b,1} + \delta \beta^2 \mathbf{h} + \sigma_{a,c} \mathbf{h} + \sigma_{b,1} \mathbf{h} + \sigma_{b,2} \beta^2 \mathbf{h}, \end{aligned} \quad (50)$$

for $l = \min\{k, r + 1\}$, with C positive constant, independent of u and of \mathbf{h} .

Proof. Using the notation of the proof of Lemma 6.4, triangle inequality implies

$$\begin{aligned} & \|\sqrt{a} \nabla e\|^2 + \|\sqrt{c_0}(u - u_h)\|^2 + \|\sqrt{\sigma_D} e\|_{\Gamma_D}^2 + \frac{1}{2} \|\sqrt{|\mathbf{b} \cdot \mathbf{n}|}(u - u_h)\|_{\Gamma_D^-}^2 \\ & + \frac{1}{2} \|\sqrt{|\mathbf{b} \cdot \mathbf{n}|}[u - u_h]\|_{\Gamma_{\text{int}}}^2 + \frac{1}{2} \|\sqrt{|\mathbf{b} \cdot \mathbf{n}|}(u - u_h)\|_{\Gamma_N^+}^2 + \|\sqrt{\delta \mathbf{h}}(\mathbf{b} \cdot \nabla_h(u - u_h))\|^2 \\ & + s_h^{a,c}(u - u_h, u - u_h) + s_h^b(u - u_h, u - u_h) \\ & \leq \left(2\|\sqrt{a} \nabla(u - \mathcal{E}(\Pi u))\|^2 + 2\|\sqrt{c_0} \eta\|^2 + 2\|\sqrt{\sigma_D}(u - \mathcal{E}(\Pi u))\|_{\Gamma_D}^2 \right. \\ & \quad + \|\sqrt{|\mathbf{b} \cdot \mathbf{n}|} \eta\|_{\Gamma_D^-}^2 + \|\sqrt{|\mathbf{b} \cdot \mathbf{n}|}[\eta]\|_{\Gamma_{\text{int}}}^2 + \|\sqrt{|\mathbf{b} \cdot \mathbf{n}|} \eta\|_{\Gamma_N^+}^2 + 2\|\sqrt{\delta \mathbf{h}}(\mathbf{b} \cdot \nabla_h \eta)\|^2 \\ & \quad \left. + 2s_h^{a,c}(\eta, \eta) + 2s_h^b(\eta, \eta) \right) + \left(2\|\xi\|_s^2 \right) =: \text{I} + \text{II}. \end{aligned} \quad (51)$$

The optimal approximation properties of L^2 -orthogonal projection operator, combined with Lemma (3.1), yield

$$\text{I} \leq C \sum_{T \in \mathcal{T}} \left(\alpha + \sigma_D \mathbf{h} + \mathbf{h}(\mathbf{h} \|c_0\|_{L^\infty(\Omega)} + \beta + \delta \beta^2 + \sigma_{a,c} + \sigma_{b,1} + \sigma_{b,2} \beta^2) \right) \mathbf{h}^{2l-2} |u|_{l,T}^2. \quad (52)$$

Next, the inf-sup condition given in Theorem 6.1 along with Lemma 6.4 give

$$\begin{aligned} \text{II} & \leq \frac{4}{\Lambda^2} \left(2\|\sqrt{a} \nabla(u - \mathcal{E}(\Pi u))\|^2 + C(r) / \sigma_{b,1} \|\sqrt{\mathbf{h}} \mathbf{b} \cdot \nabla_h \eta\|^2 + C(r) \beta / \sigma_{b,1} \|\sqrt{|\mathbf{b} \cdot \mathbf{n}|} \eta\|_{\Gamma_D^-}^2 \right. \\ & \quad + C(r) \beta / \sigma_{b,1} \|\sqrt{|\mathbf{b} \cdot \mathbf{n}|}[\eta]\|_{\Gamma_{\text{int}}}^2 + \|\sqrt{|\mathbf{b} \cdot \mathbf{n}|} \eta\|_{\Gamma_N^+}^2 + \|\sqrt{|\mathbf{b} \cdot \mathbf{n}|} \eta^-\|_{\Gamma_{\text{int}}}^2 \\ & \quad + \gamma^2 (\gamma_0^{-1} + C(r) \mathbf{h} / \sigma_{b,1}) \|u - \mathcal{E}(\Pi u)\|^2 + \|\mathbf{b}\|_{W^{1,\infty}(\Omega)}^2 / \gamma_0^2 \|\sqrt{c_0} \eta\|^2 \\ & \quad \left. + \|a \nabla(u - \mathcal{E}(\Pi u))\|_{\Gamma_D}^{-1/2} \|^2 + C(r) \|\sqrt{\sigma_D}(u - \mathcal{E}(\Pi u))\|_{\Gamma_D}^2 + s_h^{a,c}(\eta, \eta) + s_h^b(\eta, \eta) \right) \\ & \leq C \sum_{T \in \mathcal{T}} \left(\alpha + \beta^2 \mathbf{h} / \sigma_{b,1} + \beta \mathbf{h} + (\gamma^2 / \gamma_0) \mathbf{h}^2 + \|\mathbf{b}\|_{W^{1,\infty}(\Omega)}^2 \|c_0\|_{L^\infty(\Omega)} / \gamma_0^2 \mathbf{h}^2 \right. \\ & \quad \left. + \gamma^2 C(r) \mathbf{h}^3 / \sigma_{b,1} + \alpha^2 \mathbf{h}^{-1} \sigma_D^{-1} + \mathbf{h} \sigma_D + \sigma_{a,c} \mathbf{h} + \sigma_{b,1} \mathbf{h} + \sigma_{b,2} \beta^2 \mathbf{h} \right) \mathbf{h}^{2l-2} |u|_{l,T}^2. \end{aligned} \quad (53)$$

The result then follows by combining the bounds (52) and (53). \square

Remark 6.6 We note that the above a-priori error bound for RFEM (48) is optimal with respect to the mesh-size h . If $\mathbf{b} = \mathbf{0}$, the error bound (48) reduces to

$$\|\sqrt{a} \nabla(u - \mathcal{E}(u_h))\|^2 + \|\sqrt{\sigma_D}(u - \mathcal{E}(u_h))\|_{\Gamma_D}^2 + s_h^{a,0}(u - u_h, u - u_h) \leq C \mathbf{h}^{2l-2} |u|_l^2.$$

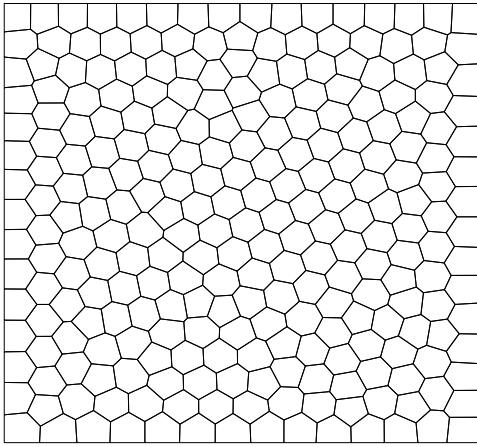
The above error bound is h -optimal and coincides the error bound from [21] which was shown for standard meshes consisting of simplices. On the other hand, if in the pure hyperbolic case with diffusion tensor $a = 0$, we deduce the error bound

$$\|u - u_h\|_b^2 + \|\sqrt{\delta \mathbf{h}}(\mathbf{b} \cdot \nabla_h(u - u_h))\|^2 + s_h^{0,c}(u - u_h, u - u_h) + s_h^b(u - u_h, u - u_h) \leq C \mathbf{h}^{2l-1} |u|_l^2,$$

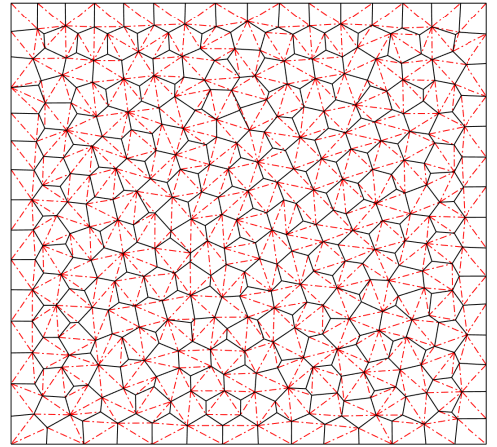
which is also h -optimal.

7 Numerical experiments

We shall now investigate numerically the asymptotic behaviour of the proposed R-FEM method on general polygonal meshes. We first introduce a sequence of polygonal meshes, indexed by their element size, together with the simplicial sub-meshes used; see Figure 1(a) for an example or 2 for a refinement of the latter. We point out that the sub-triangulations used do not introduce any new points in the interior of the polygonal mesh to keep the number of degrees of freedom in the triangulated sub-meshes to a minimum. As expected from the theory, we have numerically observed that increasing the number of degrees of freedom in the sub-meshes as a proportion of the polytopic meshes does not increase the order of the method and only improves the accuracy marginally. All the polygonal meshes are generated by PolyMesher, cf. [35]. Unless clearly stated, the R-FEM solution u_h is computed by (23) with the following choices of stabilisation parameters C_σ appearing in σ_D , $\sigma_{a,c}$ in (24), $\sigma_{b,1}$ and $\sigma_{b,2}$ in (25), all with value equal to 10.



(a) \mathcal{T} with 256 polygons.



(b) 966-triangle sub-mesh.

Figure 2: An example of a polytopic mesh \mathcal{T} which is a refinement of the mesh from Figure 1.

7.1 Example 1: a first order hyperbolic problem

Let $\Omega := (0, 1)^2$, and choose

$$a \equiv 0, \quad \mathbf{b} = (2 - y^2, 2 - x), \quad c = 1 + (1 + x)(1 + y)^2; \quad (54)$$

the forcing function f is selected so that the analytical solution to (1) is given by

$$u(x, y) = 1 + \sin(\pi(1 + x)(1 + y)^2/8), \quad (55)$$

cf. [25, 7].

We examine the convergence behaviour of the R-FEM with respect to h -refinement, with fixed polynomial r , for $r = 1, \dots, 4$. In Figure 3 the error in two different norms, against the square root of the number of degrees of freedom in the underlying finite element space V_h^r is given. The slope of the convergence rate shown is the slope of the last line segment for each convergence line. We observe that $\|u - u_h\|$ and $\|u - u_h\|_b$ converge to zero at the optimal rates $\mathcal{O}(h^{r+1})$ and at least $\mathcal{O}(h^{r+\frac{1}{2}})$, respectively, as the mesh size h tends to zero for each fixed r . The latter results agree with the result (48) in Theorem 6.5. Notice that the behaviour of

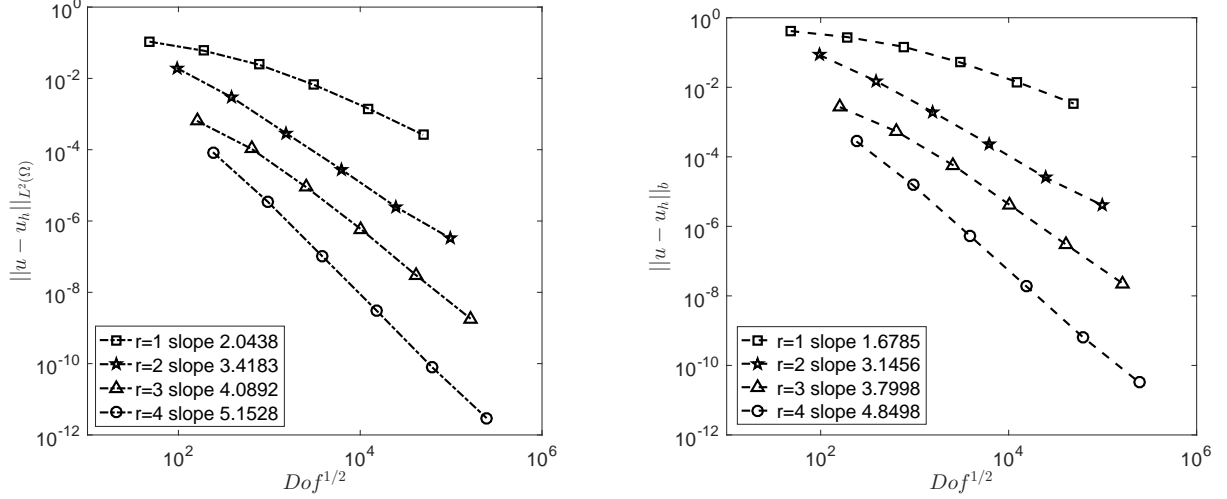


Figure 3: Example 1. Error against numerical degrees of freedom (Dof). Here we examine the convergence of the R-FEM under h -refinement for polynomial degrees $r = 1, 2, 3, 4$. Notice that $\|u - u_h\|_{L^2(\Omega)} = O(h^{r+1})$, which is optimal. In addition, $\|u - u_h\|_b$ appears to converge faster than the analysis of Theorem 6.5 suggests for even polynomial degrees.

$\|u - u_h\|_b$ appears to differ as to whether r is odd or even. This is well documented in the study of discontinuous Galerkin methods for hyperbolic conservation laws [13, 22] and seems to be a feature of the above R-FEM method as well.

7.2 Example 2: a nonsymmetric elliptic problem

Let $\Omega := (0, 1)^2$, and choose

$$a \equiv 1, \quad \mathbf{b} = (1 - y, 1 - x), \quad c \equiv 2; \quad (56)$$

the forcing function f is selected so that the analytical solution to (1) is given by

$$u(x, y) = \sin(\pi x) \sin(\pi y). \quad (57)$$

We examine the convergence behaviour of the R-FEM with respect to h -refinement on quasi-uniform polygonal meshes, with fixed polynomial r , for $r = 1, \dots, 4$. In Figure 4 we plot the error, in terms of the L^2 -norm and the (broken) H^1 -seminorm for both discontinuous R-FEM approximation u_h and the conforming R-FEM approximation $\mathcal{E}(u_h)$, against the square root of the number of degrees of freedom in the underlying finite element space V_h^r . We observe that $\|u - u_h\|$ and $|u - u_h|_{H^1(\Omega, \mathcal{T})}$ converge to zero at the optimal rates $\mathcal{O}(h^{r+1})$ and $\mathcal{O}(h^r)$, respectively, as the mesh size h tends to zero for each fixed r . Moreover, the difference between the R-FEM solutions u_h and $\mathcal{E}(u_h)$ is marginal. The results are in accordance with Theorem 6.5.

7.3 Example 3: a advection-dominated elliptic problem

We now investigate the numerical stability of the R-FEM through a series of advection-dominated elliptic problems. Let $\Omega := (0, 1)^2$, and choose

$$a \equiv \epsilon, \quad \mathbf{b} = (1, 1), \quad c \equiv 0; \quad (58)$$

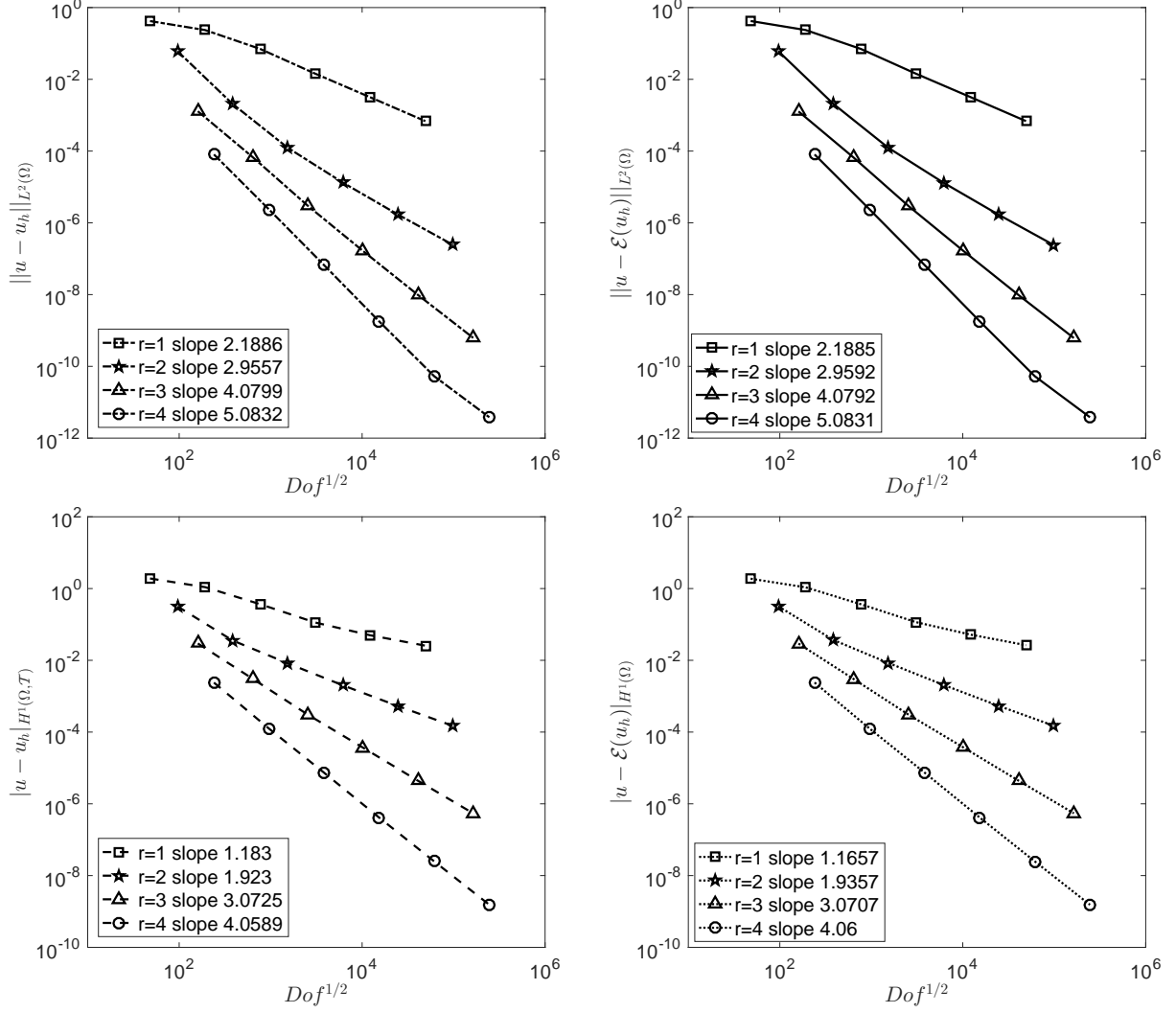


Figure 4: Example 2. Convergence of the R-FEM under h -refinement for $r = 1, 2, 3, 4$.

together with a forcing function $f = 1$ and homogeneous Dirichlet boundary conditions. This example is known to admit boundary layers in the vicinity of the right and top boundaries $x = 1$ and $y = 1$ when $\epsilon \ll 1$. We investigate the stability of R-FEM as $\epsilon \rightarrow 0$ on a fixed, relatively coarse mesh which is insufficient to resolve the layer. More specifically, we consider a fixed mesh consisting of 1024 polygons over the domain, we choose $r = 1$ and take $\epsilon = 10^{-2}, 10^{-4}, 10^{-6}$. In Figure 5 we plot the numerical solutions u_h and $\mathcal{E}(u_h)$. We observe that for $\epsilon = 10^{-2}$, the mesh is fine enough to resolve the layer and, hence, both u_h and $\mathcal{E}(u_h)$ are stable. For $\epsilon = 10^{-4}$, the mesh is no longer fine enough to resolve the layer. However, the solutions are still stable in the sense that neither solution admits non-physical oscillations near the boundary. In the case $\epsilon = 10^{-6}$, the mesh is too coarse to resolve the layer. Both u_h and $\mathcal{E}(u_h)$ appear to be stable in this case. Moreover, the solutions are very close to the solution for the pure hyperbolic problem with inflow boundary satisfying Dirichlet boundary conditions. This is expected as the boundary conditions have been imposed in a weak fashion for the numerical method to be valid in the hyperbolic limit $\epsilon = 0$ also, in the spirit of the classical discontinuous Galerkin methods.

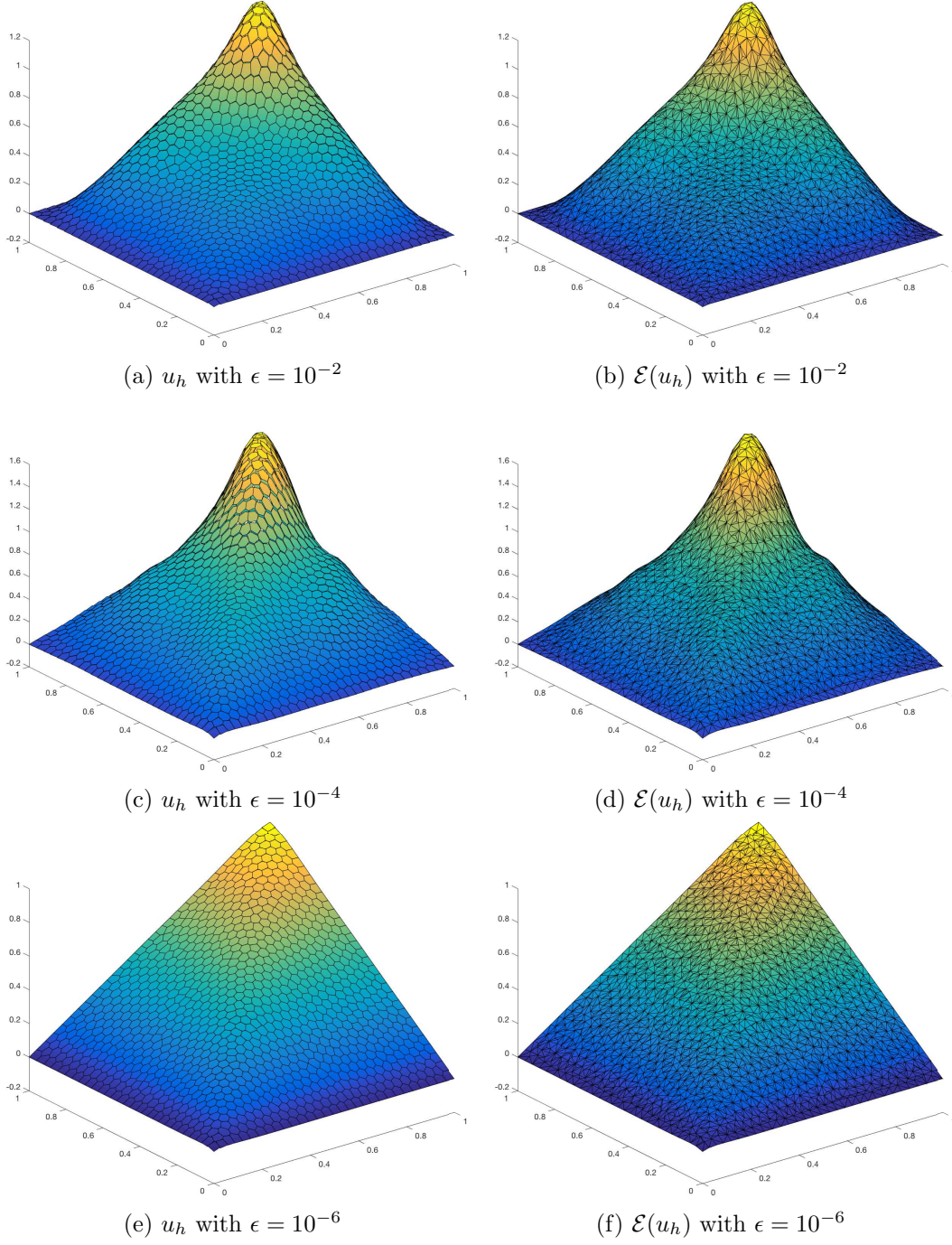


Figure 5: Example 3. R-FEM solutions for a mesh consisting of 1024 polygonal elements and $r = 1$.

7.4 Example 4 – a mixed-type problem

We now consider a partial differential equation with nonnegative characteristic form of mixed type. To this end, we let $\Omega = (-1, 1)^2$, and consider the PDE problem:

$$\begin{cases} -x^2 u_{yy} + u_x + u = 0, & \text{for } -1 \leq x \leq 1, y > 0, \\ u_x + u = 0, & \text{for } -1 \leq x \leq 1, y \leq 0, \end{cases} \quad (59)$$

with analytical solution:

$$u(x, y) = \begin{cases} \sin(\frac{1}{2}\pi(1+y)) \exp(-(x + \frac{\pi^2 x^3}{12})), & \text{for } -1 \leq x \leq 1, y > 0, \\ \sin(\frac{1}{2}\pi(1+y)) \exp(-x), & \text{for } -1 \leq x \leq 1, y \leq 0, \end{cases} \quad (60)$$

cf. [7]. This problem is hyperbolic in the region $y \leq 0$ and parabolic for $y > 0$. Notice that, in order to ensure continuity of the normal flux across $y = 0$ where the partial differential equation changes type, the analytical solution has a discontinuity across the line $y = 0$, cf. [25].

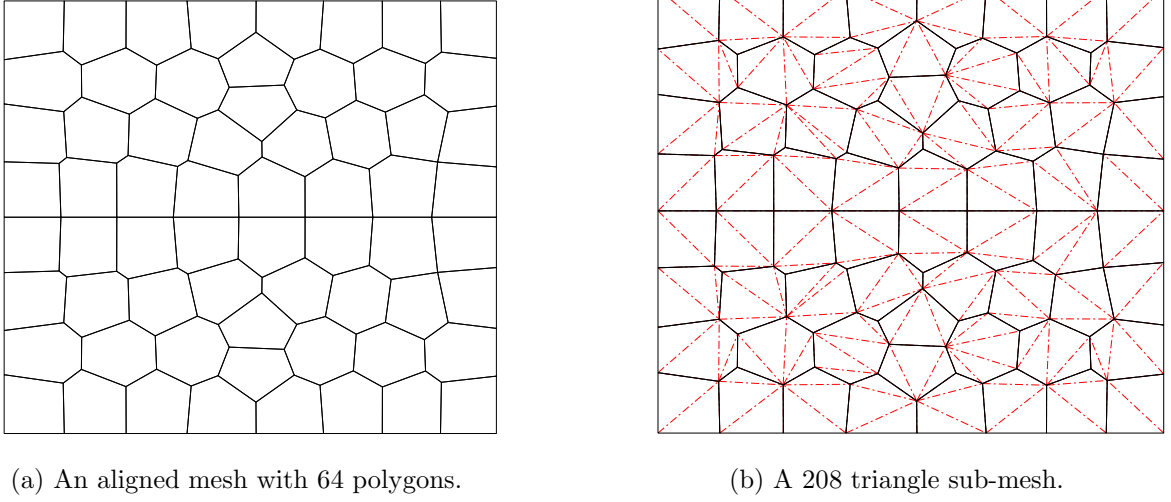


Figure 6: An aligned polytopic mesh, \mathcal{T} , with 64 polygons and 208 triangle sub-mesh $\tilde{\mathcal{T}}$.

We examine the convergence behaviour of the R-FEM with respect to h -refinement, with fixed polynomial r , for $r = 1, \dots, 4$. To have the opportunity to possibly observe optimal convergence rates, we align the polygonal mesh with the solution's discontinuity; a typical mesh is shown in Figure 6. Also, for this example the recovery operator is constructed in piecewise fashion over the two subdomains. This ensures the conforming R-FEM solution $\mathcal{E}(u_h)$ is able to have a jump discontinuity over the interface where the problem changes type.

In Figure 7 we plot the L^2 -norm error, as well as the error in the norm on the left hand-side of (48) for R-FEM approximation u_h , against the square root of the number of degrees of freedom in the underlying finite element space V_h^r . Abusing the notation, we use again $\|\cdot\|_s$ to denote the norm on the left hand-side of (48). We observe that $\|u - u_h\|_s$ converges to zero at the optimal rates $\mathcal{O}(h^r)$, as the mesh size h tends to zero for each fixed r . These results agree with the result (48) in Theorem 6.5. However, the convergence rate for $\|u - u_h\|$ seems to be slightly suboptimal in h . Additionally, we also plot the error in terms of L^2 -norm and H^1 -seminorm for $\mathcal{E}(u_h)$, against the square root of the number of degrees of freedom in the underlying finite element space V_h^r . Here, again, observe that $\|u - \mathcal{E}(u_h)\|$ and $|u - \mathcal{E}(u_h)|_{H^1\Omega}$ converge to zero at a slightly suboptimal rate.

Acknowledgements

We wish to express our sincere gratitude Andrea Cangiani (University of Leicester) for his insightful comments on an earlier version of this work. ZD and EHG acknowledge funding by The Leverhulme Trust (grant no. RPG-2015-306) and TP acknowledges funding by the EPSRC grant EP/P000835/1.

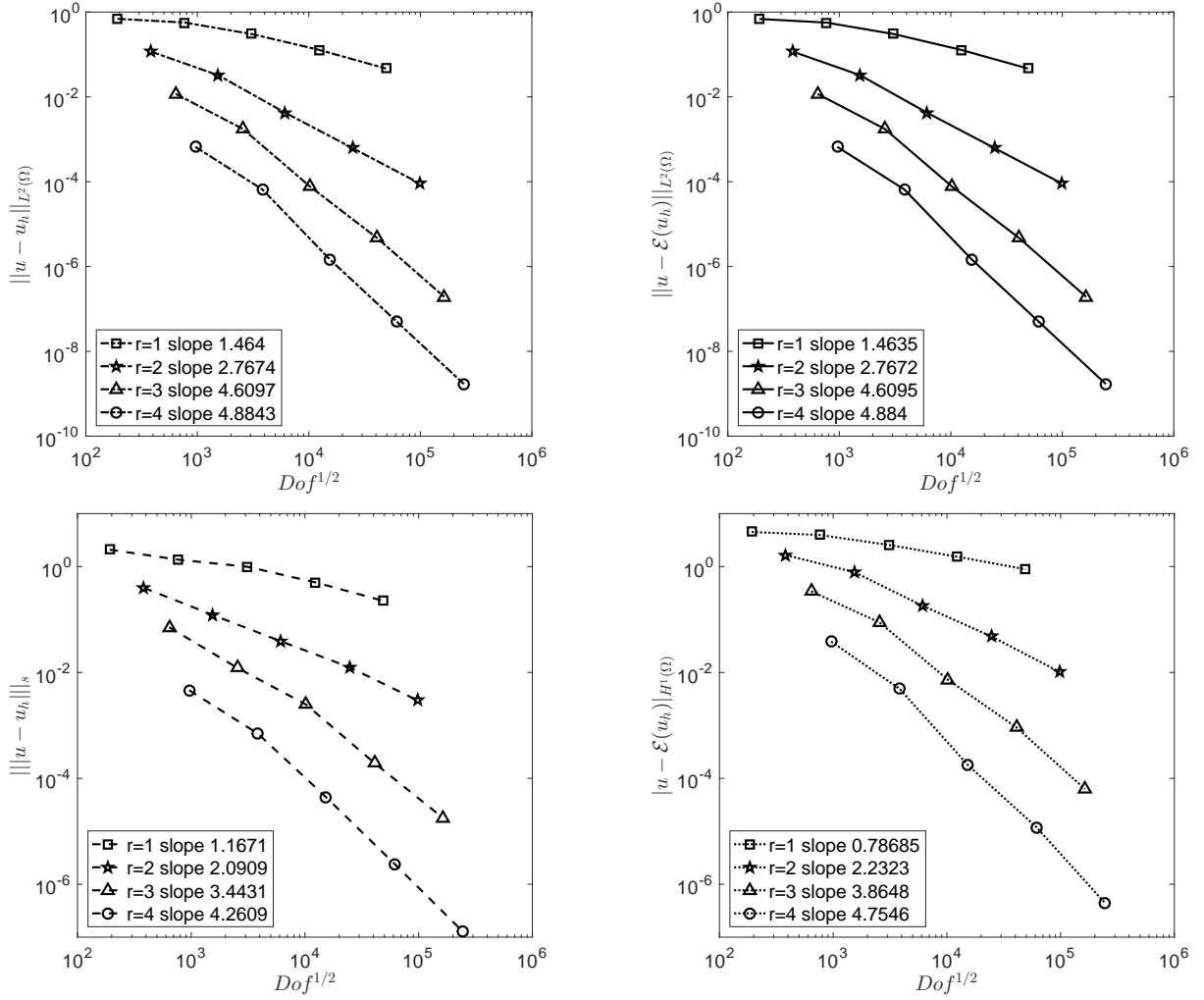


Figure 7: Example 4. Convergence of the R-FEM under h -refinement for $r = 1, 2, 3, 4$.

References

- [1] L. BEIRÃO DA VEIGA, K. LIPNIKOV, AND G. MANZINI, *The mimetic finite difference method for elliptic problems*, vol. 11 of MS&A. Modeling, Simulation and Applications, Springer, Cham, 2014.
- [2] L. BEIRÃO DA VEIGA, F. BREZZI, A. CANGIANI, G. MANZINI, L. MARINI, AND A. RUSSO, *Basic principles of virtual element methods*, Math. Models Methods Appl. Sci., 23 (2013), pp. 199–214.
- [3] S. C. BRENNER AND L.-Y. SUNG, *C^0 interior penalty methods for fourth order elliptic boundary value problems on polygonal domains*, J. Sci. Comput., 22/23 (2005), pp. 83–118.
- [4] E. BURMAN, *A unified analysis for conforming and nonconforming stabilized finite element methods using interior penalty*, SIAM J. Numer. Anal., 43 (2005), pp. 2012–2033.
- [5] E. BURMAN AND P. HANSBO, *Edge stabilization for Galerkin approximations of convection-diffusion-reaction problems*, Comput. Methods Appl. Mech. Engrg., 193 (2004), pp. 1437–1453.

- [6] A. CANGIANI, Z. DONG, AND E. H. GEORGOULIS, *hp-version space-time discontinuous galerkin methods for parabolic problems on prismatic meshes*, SIAM J. Sci. Comput., 39 (2017), pp. A1251–A1279.
- [7] A. CANGIANI, Z. DONG, E. H. GEORGOULIS, AND P. HOUSTON, *hp-version discontinuous Galerkin methods for advection-diffusion-reaction problems on polytopic meshes*, ESAIM Math. Model. Numer. Anal., 50 (2016), pp. 699–725.
- [8] ———, *hp-Version Discontinuous Galerkin Methods on Polygonal and Polyhedral Meshes*, Springer, 2017.
- [9] A. CANGIANI, E. H. GEORGOULIS, AND P. HOUSTON, *hp-version discontinuous Galerkin methods on polygonal and polyhedral meshes*, Math. Models Methods Appl. Sci., 24 (2014), pp. 2009–2041.
- [10] A. CANGIANI, G. MANZINI, AND O. J. SUTTON, *Conforming and nonconforming virtual element methods for elliptic problems*, IMA J. Numer. Anal., 37 (2017), pp. 1317–1354.
- [11] P. G. CIARLET, *The finite element method for elliptic problems*, vol. 40 of Classics in Applied Mathematics, Society for Industrial and Applied Mathematics (SIAM), Philadelphia, PA, 2002.
- [12] P. CLÉMENT, *Approximation by finite element functions using local regularization*, RAIRO Analyse Numérique, 9 (1975), pp. 77–84.
- [13] B. COCKBURN, *Continuous dependence and error estimation for viscosity methods*, Acta Numerica, 12 (2003), pp. 127–180.
- [14] B. COCKBURN, D. DI PIETRO, AND A. ERN, *Bridging the hybrid high-order and hybridizable discontinuous Galerkin methods*, ESAIM Math. Model. Numer. Anal., 50 (2016), pp. 635–650.
- [15] B. COCKBURN, J. GOPALAKRISHNAN, AND R. LAZAROV, *Unified hybridization of discontinuous Galerkin, mixed, and continuous Galerkin methods for second order elliptic problems*, SIAM J. Numer. Anal., 47 (2009), pp. 1319–1365.
- [16] D. DI PIETRO AND A. ERN, *Mathematical aspects of discontinuous Galerkin methods*, vol. 69 of Mathématiques & Applications (Berlin) [Mathematics & Applications], Springer, Heidelberg, 2012.
- [17] J. DOUGLAS, JR. AND T. DUPONT, *Interior penalty procedures for elliptic and parabolic Galerkin methods*, (1976), pp. 207–216. Lecture Notes in Phys., Vol. 58.
- [18] E. GEORGOULIS, C. MAKRIDAKIS, AND T. PRYER, *Babuška-Osborn techniques in discontinuous Galerkin methods: L^2 -norm error estimates for unstructured meshes*, arXiv preprint arXiv:1704.05238, (2017).
- [19] E. H. GEORGOULIS, P. HOUSTON, AND J. VIRTANEN, *An a posteriori error indicator for discontinuous Galerkin approximations of fourth-order elliptic problems*, IMA J. Numer. Anal., 31 (2011), pp. 281–298.
- [20] E. H. GEORGOULIS AND A. LASIS, *A note on the design of hp-version interior penalty discontinuous Galerkin finite element methods for degenerate problems.*, IMA J. Numer. Anal., 26 (2006), pp. 381–390.

- [21] E. H. GEORGOULIS AND T. PRYER, *Recovered finite element methods*, Comput. Methods Appl. Mech. Engrg., 332 (2018), pp. 303 – 324.
- [22] J. GIESSELMANN, C. MAKRIDAKIS, AND T. PRYER, *A posteriori analysis of discontinuous galerkin schemes for systems of hyperbolic conservation laws*, SIAM Journal on Numerical Analysis, 53 (2015), pp. 1280–1303.
- [23] W. HACKBUSCH AND S. SAUTER, *Composite finite elements for the approximation of PDEs on domains with complicated micro-structures*, Numer. Math., 75 (1997), pp. 447–472.
- [24] P. HOUSTON, C. SCHWAB, AND E. SÜLI, *Stabilized hp-finite element methods for first-order hyperbolic problems*, SIAM J. Numer. Anal., 37 (2000), pp. 1618–1643.
- [25] ———, *Discontinuous hp-finite element methods for advection-diffusion-reaction problems*, SIAM J. Numer. Anal., 39 (2002), pp. 2133–2163.
- [26] P. HOUSTON AND E. SÜLI, *Stabilised hp-finite element approximation of partial differential equations with nonnegative characteristic form*, Computing, 66 (2001), pp. 99–119.
- [27] O. A. KARAKASHIAN AND F. PASCAL, *Convergence of adaptive discontinuous Galerkin approximations of second-order elliptic problems*, SIAM J. Numer. Anal., 45 (2007), pp. 641–665 (electronic).
- [28] J. NITSCHKE, *über ein Variationsprinzip zur Lösung von Dirichlet-Problemen bei Verwendung von Teilräumen, die keinen Randbedingungen unterworfen sind*, Abh. Math. Sem. Univ. Hamburg, 36 (1971), pp. 9–15. Collection of articles dedicated to Lothar Collatz on his sixtieth birthday.
- [29] O. OLEINIK AND E. RADKEVIČ, *Second Order Equations with Nonnegative Characteristic Form*, American Mathematical Society, 1973.
- [30] P. OSWALD, *On a BPX-preconditioner for P1 elements*, Computing, 51 (1993), pp. 125–133.
- [31] D. PETERSEIM AND S. A. SAUTER, *The composite mini element-coarse mesh computation of Stokes flows on complicated domains*, SIAM J. Numer. Anal., 46 (2008), pp. 3181–3206.
- [32] W. REED AND T. HILL, *Triangular mesh methods for the neutron transport equation.*, Technical Report LA-UR-73-479 Los Alamos Scientific Laboratory, (1973).
- [33] L. R. SCOTT AND S. ZHANG, *Finite element interpolation of nonsmooth functions satisfying boundary conditions*, Math. Comp., 54 (1990), pp. 483–493.
- [34] N. SUKUMAR AND A. TABARRAEI, *Conforming polygonal finite elements*, Internat. J. Numer. Methods Engrg., 61 (2004), pp. 2045–2066.
- [35] C. TALISCHI, G. PAULINO, A. PEREIRA, AND I. MENEZES, *Polymesher: A general-purpose mesh generator for polygonal elements written in Matlab*, Struct. Multidisc. Optim., 45 (2012), pp. 309–328.